

**The protonmotive force and respiratory control:
Building blocks of mitochondrial physiology
Part 1.**

http://www.mitoeagle.org/index.php/MitoEAGLE_preprint_2017-09-21

Preprint version 16 (2017-11-11)

MitoEAGLE Network

Corresponding author: Gnaiger E

Contributing co-authors

Ahn B, Alves MG, Amati F, Åsander Frostner E, Bailey DM, Bastos Sant'Anna Silva AC, Battino M, Beard DA, Ben-Shachar D, Bishop D, Breton S, Brown GC, Brown RA, Buettner GR, Carvalho E, Cervinkova Z, Chang SC, Chicco AJ, Coen PM, Collins JL, Crisóstomo L, Davis MS, Dias T, Distefano G, Doerrier C, Ehinger J, Elmer E, Fell DA, Ferko M, Ferreira JCB, Filipovska A, Fisar Z, Fisher J, Garcia-Roves PM, Garcia-Souza LF, Genova ML, Gonzalo H, Goodpaster BH, Gorr TA, Han J, Harrison DK, Hellgren KT, Hernansanz P, Holland O, Hoppel CL, Iglesias-Gonzalez J, Irving BA, Iyer S, Jackson CB, Jansen-Dürr P, Jespersen NR, Jha RK, Kaambre T, Kane DA, Kappler L, Keijer J, Komlodi T, Kopitar-Jerala N, Krako Jakovljevic N, Kuang J, Labieniec-Watala M, Lai N, Laner V, Lee HK, Lemieux H, Lerfall J, Lucchinetti E, MacMillan-Crow LA, Makrecka-Kuka M, Meszaros AT, Moiso N, Molina AJA, Montaigne D, Moore AL, Murray AJ, Newsom S, Nozickova K, O'Gorman D, Oliveira PF, Oliveira PJ, Orynbayeva Z, Pak YK, Palmeira CM, Patel HH, Pesta D, Petit PX, Pichaud N, Pirkmajer S, Porter RK, Pranger F, Prochownik EV, Radenkovic F, Reboredo P, Renner-Sattler K, Robinson MM, Rohlena J, Røslund GV, Rossiter HB, Salvadego D, Scatena R, Schartner M, Scheibye-Knudsen M, Schilling JM, Schlattner U, Schoenfeld P, Scott GR, Singer D, Sobotka O, Spinazzi M, Stier A, Stocker R, Sumbalova Z, Suravajhala P, Tanaka M, Tandler B, Tepp K, Tomar D, Towheed A, Trivigno C, Tronstad KJ, Trougakos IP, Tyrrell DJ, Velika B, Vendelin M, Vercesi AE, Victor VM, Wagner BA, Ward ML, Watala C, Wei YH, Wieckowski MR, Wohlwend M, Wolff J, Wuest RCI, Zaugg K, Zaugg M, Zorzano A

Supporting co-authors:

Arandarčikaitė O, Bakker BM, Bernardi P, Boetker HE, Borsheim E, Borutaitė V, Bouitbir J, Calabria E, Calbet JA, Chaurasia B, Clementi E, Coker RH, Collin A, Das AM, De Palma C, Dubouchaud H, Duchon MR, Durham WJ, Dyrstad SE, Engin AB, Fornaro M, Gan Z, Garland KD, Garten A, Gourlay CW, Granata C, Haas CB, Haavik J, Haendeler J, Hand SC, Hepple RT, Hickey AJ, Hoel F, Kainulainen H, Keppner G, Khamoui AV, Klingenspor M, Koopman WJH, Kowaltowski AJ, Krajcova A, Lenaz G, Malik A, Markova M, Mazat JP, Menze MA, Methner A, Mracek T, Muntané J, Muntean DM, Neuzil J, Oliveira MT, Pallotta ML, Parajuli N, Pettersen IKN, Porter C, Pulinilkunnil T, Ropelle ER, Salin K, Sandi C, Sazanov LA, Siewiera K, Silber AM, Skolik R, Smenes BT, Soares FAA, Sokolova I, Sonkar VK, Stankova P, Swerdlow RH, Szabo I, Trifunovic A, Thyfault JP, Tretter L, Valentine JM, Vieyra A, Votion DM, Williams C

Updates:

http://www.mitoeagle.org/index.php/MitoEAGLE_preprint_2017-09-21

Correspondence: Gnaiger E

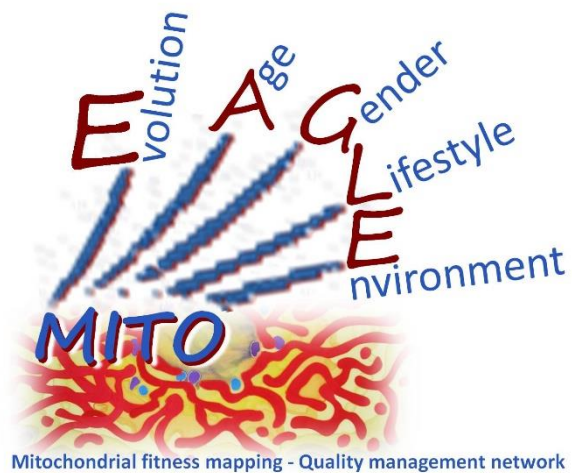
Department of Visceral, Transplant and Thoracic Surgery, D. Swarovski Research Laboratory, Medical University of Innsbruck, Innrain 66/4, A-6020 Innsbruck, Austria

Email: erich.gnaiger@i-med.ac.at

Tel: +43 512 566796, Fax: +43 512 566796 20

This manuscript on 'The protonmotive force and respiratory control' is a position statement in the frame of COST Action CA15203 MitoEAGLE. The list of co-authors evolved beyond **phase 1** in the **bottom-up** spirit of COST (phase 1 versions 1-44).

This is an open invitation to scientists and students to join as co-authors, to provide a balanced view on mitochondrial respiratory control, a fundamental introductory presentation of the concept of the protonmotive force, and a consensus statement on reporting data of mitochondrial respiration in terms of metabolic flows and fluxes.



Phase 2: MitoEAGLE preprint (Versions 01 – 15): We continue to invite comments and suggestions, particularly if you are an **early career investigator adding an open future-oriented perspective**, or an **established scientist providing a balanced historical basis**. Your critical input into the quality of the manuscript will be most welcome, improving our aims to be educational, general, consensus-oriented, and practically helpful for students working in mitochondrial respiratory physiology.

Phase 3 (2017-11-11) Print version for MiP2017 and MitoEAGLE workshop in Hradec Kralove: Discuss manuscript submission to a preprint server, such as BioRxiv; invite further **opinion leaders:** To join as a co-author, please feel free to focus on a particular section in terms of direct input and references, contributing to the scope of the manuscript from the perspective of your expertise. Your comments will be largely posted on the discussion page of the MitoEAGLE preprint website.

If you prefer to submit comments in the format of a referee's evaluation rather than a contribution as a co-author, I will be glad to distribute your views to the updated list of co-authors for a balanced response. We would ask for your consent on this open bottom-up policy.

We organize a MitoEAGLE session on the manuscript at the MiPconference/MitoEAGLE WG Meeting Nov 2017 in Hradec Kralove in close association with the MiPsociety:

» http://www.mitoeagle.org/index.php/MiP2017_Hradec_Kralove_CZ

Phase 4: Journal submission. We plan a series of follow-up reports by the expanding MitoEAGLE Network, to increase the scope of recommendations on harmonization and facilitate global communication and collaboration. Further discussions: MitoEAGLE Working Group Meetings, various conferences (EBEC 2018 in Budapest).

I thank you in advance for your feedback.

With best wishes,

Erich Gnaiger

Chair Mitochondrial Physiology Society - <http://www.mitophysiology.org>

Chair COST Action MitoEAGLE - <http://www.mitoeagle.org>

101	Contents
102	1. Introduction
103	2. Respiratory coupling states in mitochondrial preparations
104	Mitochondrial preparations
105	2.1. <i>Three coupling states of mitochondrial preparations and residual oxygen consumption</i>
106	Coupling control states and respiratory capacities
107	Kinetic control
108	Phosphorylation, P \gg
109	LEAK, OXPHOS, ET, ROX
110	2.2. <i>Coupling states and respiratory rates</i>
111	2.3. <i>Classical terminology for isolated mitochondria</i>
112	States 1-5
113	3. The protonmotive force and proton flux
114	3.1. <i>Electric and chemical partial forces versus electrical and chemical units</i>
115	Faraday constant
116	Electric part of the protonmotive force
117	Chemical part of the protonmotive force
118	3.2. <i>Definitions</i>
119	Control and regulation
120	Respiratory control and response
121	Respiratory coupling control
122	Pathway control states
123	The steady-state
124	3.3. <i>Forces and fluxes in physics and thermodynamics</i>
125	Vectorial and scalar forces, and fluxes
126	Coupling
127	Coupled versus bound processes
128	4. Normalization: fluxes and flows
129	4.1. <i>Flux per chamber volume</i>
130	4.2. <i>System-specific and sample-specific normalization</i>
131	Extensive quantities
132	Size-specific quantities
133	Molar quantities
134	Flow per system, I
135	Size-specific flux, J
136	Sample concentration, C_{mX}
137	Mass-specific flux, J_{mX,O_2}
138	Number concentration, C_{NX}
139	Flow per sample entity, I_{X,O_2}
140	4.3. <i>Normalization for mitochondrial content</i>
141	Mitochondrial concentration, C_{mte} , and mitochondrial markers
142	Mitochondria-specific flux, J_{mte,O_2}
143	4.4. <i>Conversion: units and normalization</i>
144	4.5. <i>Conversion: oxygen, proton and ATP flux</i>
145	5. Conclusions
146	6. References
147	

148 **Abstract** Clarity of concept and consistency of nomenclature are key trademarks of a research
 149 field. These trademarks facilitate effective transdisciplinary communication, education, and
 150 ultimately further discovery. As the knowledge base and importance of mitochondrial
 151 physiology to human health expand, the necessity for harmonizing nomenclature concerning
 152 mitochondrial respiratory states and rates has become increasingly apparent. Peter Mitchell's
 153 chemiosmotic theory establishes the links between electrical and chemical components of
 154 energy transformation and coupling in oxidative phosphorylation. This unifying concept of the
 155 protonmotive force provides the framework for developing a consistent nomenclature for
 156 mitochondrial physiology and bioenergetics. Herein, we follow IUPAC guidelines on general
 157 terms of physical chemistry, extended by the concepts of open systems and irreversible
 158 thermodynamics. We align the nomenclature of classical bioenergetics on respiratory states
 159 with a concept-driven constructive terminology to address the meaning of each respiratory state.
 160 Furthermore, we suggest uniform standards for the evaluation of respiratory states that will
 161 ultimately support the development of databases of mitochondrial respiratory function in
 162 species, tissues and cells studied under diverse physiological and experimental conditions. In
 163 this position statement, in the frame of COST Action MitoEAGLE, we endeavour to provide a
 164 balanced view on mitochondrial respiratory control, a fundamental introductory presentation of
 165 the concept of the protonmotive force, and a critical discussion on reporting data of
 166 mitochondrial respiration in terms of metabolic flows and fluxes.

167
 168 *Keywords:* Mitochondrial respiratory control, coupling control, mitochondrial
 169 preparations, protonmotive force, chemiosmotic theory, oxidative phosphorylation, OXPHOS,
 170 efficiency, electron transfer, ET; proton leak, LEAK, residual oxygen consumption, ROX, State
 171 2, State 3, State 4, normalization, flow, flux
 172

173 **Box 1:**

174
 175 **In brief:**
 176 **mitochondria**
 177 **and Bioblasts**

- Does the public expect biologists to understand Darwin's theory of evolution?
- Do students expect that researchers of bioenergetics can explain Mitchell's theory of chemiosmotic energy transformation?

179 **Mitochondria** were described by Richard Altmann (1894) as 'bioblasts', which include not
 180 only the mitochondria as presently defined, but also symbiotic and free-living bacteria. The
 181 word 'mitochondrion' (Greek mitos: thread; chondros: granule) was introduced by Carl Benda
 182 (1898). Mitochondria are the oxygen-consuming electrochemical generators which evolved
 183 from endosymbiotic bacteria (Margulis 1970; Lane 2005).

184 We now recognize mitochondria as dynamic organelles with a double membrane that are
 185 contained within eukaryotic cells. The mitochondrial inner membrane (mtIM) shows dynamic
 186 tubular to disk-shaped cristae that separate the mitochondrial matrix, *i.e.* the internal
 187 mitochondrial compartment, and the intermembrane space; the latter being enclosed by the
 188 mitochondrial outer membrane (mtOM). Mitochondria are the structural and functional
 189 elemental units of cell respiration. Cell respiration is the consumption of oxygen by electron
 190 transfer coupled to electrochemical proton translocation across the mtIM. In the process of
 191 oxidative phosphorylation (OXPHOS), the reduction of O₂ is electrochemically coupled to the
 192 transformation of energy in the form of adenosine triphosphate (ATP; Mitchell 1961, 2011).
 193 These powerhouses of the cell contain the machinery of the OXPHOS-pathway, including
 194 transmembrane respiratory complexes (*i.e.* proton pumps with FMN, Fe-S and cytochrome *b*,
 195 *c*, *aa₃* redox systems); alternative dehydrogenases and oxidases; the coenzyme ubiquinone (Q);
 196 ATP synthase; the enzymes of the tricarboxylic acid cycle and the fatty acid oxidation enzymes;
 197 transporters of ions, metabolites and co-factors; and mitochondrial kinases related to energy
 198 transfer pathways. The mitochondrial proteome comprises over 1,200 proteins
 199 (MITOCARTA), mostly encoded by nuclear DNA (nDNA), with a variety of functions, many

200 of which are relatively well known (*e.g.* apoptosis-regulating proteins), while others are still
201 under investigation, or need to be identified (*e.g.* alanine transporter).

202 Mitochondria typically maintain several copies of their own genome (hundred to
203 thousands per cell; Cummins 1998), which is almost exclusively maternally inherited (White *et*
204 *al.* 2008) and known as mitochondrial DNA (mtDNA). One exception to strictly maternal
205 inheritance in animals is found in bivalves (Breton *et al.* 2007). mtDNA is 16.5 kB in length,
206 contains 13 protein-coding genes for subunits of the transmembrane respiratory Complexes CI,
207 CIII, CIV and ATP synthase, and also encodes 22 tRNAs and the mitochondrial 16S and 12S
208 rRNA. The mitochondrial genome is both regulated and supplemented by nuclear-encoded
209 mitochondrial targeted proteins. Evidence has accumulated that additional gene content is
210 encoded in the mitochondrial genome, *e.g.* microRNAs, piRNA, smithRNAs, repeat associated
211 RNA, and even additional proteins (Duarte *et al.* 2014; Lee *et al.* 2015; Cobb *et al.* 2016).

212 The mtIM contains the non-bilayer phospholipid cardiolipin, which is not present in any
213 other eukaryotic cellular membrane. Cardiolipin promotes the formation of respiratory
214 supercomplexes, which are supramolecular assemblies based upon specific, though dynamic,
215 interactions between individual respiratory complexes (Greggio *et al.* 2017; Lenaz *et al.* 2017).
216 Membrane fluidity is an important parameter influencing functional properties of proteins
217 incorporated in the membranes (Waczulikova *et al.* 2007). There is a constant crosstalk between
218 mitochondria and the other cellular components, maintaining cellular mitostasis through
219 regulation at both the transcriptional and post-translational level, and through cell signalling
220 including proteostatic (*e.g.* the ubiquitin-proteasome and autophagy-lysosome pathways) and
221 genome stability modules throughout the cell cycle or even cell death, contributing to
222 homeostatic regulation in response to varying energy demands and stress (Quiros *et al.* 2016).
223 In addition to mitochondrial movement along the microtubules, mitochondrial morphology can
224 change in response to the energy requirements of the cell via processes known as fusion and
225 fission, through which mitochondria can communicate within a network, and in response to
226 intracellular stress factors causing swelling and ultimately permeability transition.

227 Mitochondrial dysfunction is associated with a wide variety of genetic and degenerative
228 diseases. Robust mitochondrial function is supported by physical exercise and caloric balance,
229 and is central for sustained metabolic health throughout life. Therefore, a more consistent
230 presentation of mitochondrial physiology will improve our understanding of the etiology of
231 disease, the diagnostic repertoire of mitochondrial medicine, with a focus on protective
232 medicine, lifestyle and healthy aging.

233 Abbreviation: mt, as generally used in mtDNA. Mitochondrion is singular and
234 mitochondria is plural.

235 *‘For the physiologist, mitochondria afforded the first opportunity for an experimental*
236 *approach to structure-function relationships, in particular those involved in active transport,*
237 *vectorial metabolism, and metabolic control mechanisms on a subcellular level’* (Ernster and
238 Schatz 1981).

239

240 1. Introduction

241 Mitochondria are the powerhouses of the cell with numerous physiological, molecular,
242 and genetic functions (**Box 1**). Every study of mitochondrial function and disease is faced with
243 **E**volution, **A**ge, **G**ender and sex, **L**ifestyle, and **E**nvironment (EAGLE) as essential background
244 conditions intrinsic to the individual patient or subject, cohort, species, tissue and to some extent
245 even cell line. As a large and highly coordinated group of laboratories and researchers, the
246 mission of the global MitoEAGLE Network is to generate the necessary scale, type, and quality
247 of consistent data sets and conditions to address this intrinsic complexity. Harmonization of
248 experimental protocols and implementation of a quality control and data management system
249 is required to interrelate results gathered across a spectrum of studies and to generate a
250 rigorously monitored database focused on mitochondrial respiratory function. In this way,

251 researchers within the same and across different disciplines will be positioned to compare their
252 findings to an agreed upon set of clearly defined and accepted international standards.

253 Reliability and comparability of quantitative results depend on the accuracy of
254 measurements under strictly-defined conditions. A conceptually defined framework is also
255 required to warrant meaningful interpretation and comparability of experimental outcomes
256 carried out by research groups at different institutes. With an emphasis on quality of research,
257 collected data can be useful far beyond the specific question of a particular experiment.
258 Enabling meta-analytic studies is the most economic way of providing robust answers to
259 biological questions (Cooper *et al.* 2009). Vague or ambiguous jargon can lead to confusion
260 and may relegate valuable signals to wasteful noise. For this reason, measured values must be
261 expressed in standardized units for each parameter used to define mitochondrial respiratory
262 function. Standardization of nomenclature and definition of technical terms is essential to
263 improve the awareness of the intricate meaning of a divergent scientific vocabulary, for
264 documentation and integration into databases in general, and quantitative modelling in
265 particular (Beard 2005). The focus on the protonmotive force, coupling states, and fluxes
266 through metabolic pathways of aerobic energy transformation in mitochondrial preparations is
267 a first step in the attempt to generate a harmonized and conceptually-oriented nomenclature in
268 bioenergetics and mitochondrial physiology. Coupling states of intact cells and respiratory
269 control by fuel substrates and specific inhibitors of respiratory enzymes will be reviewed in
270 subsequent communications.

271

272 **2. Respiratory coupling states in mitochondrial preparations**

273 *‘Every professional group develops its own technical jargon for talking about*
274 *matters of critical concern ... People who know a word can share that idea with*
275 *other members of their group, and a shared vocabulary is part of the glue that holds*
276 *people together and allows them to create a shared culture’ (Miller 1991).*

277 **Mitochondrial preparations** are defined as either isolated mitochondria, or tissue and
278 cellular preparations in which the barrier function of the plasma membrane is disrupted. The
279 plasma membrane separates the cytosol, nucleus, and organelles (the intracellular
280 compartment) from the environment of the cell. The plasma membrane consists of a lipid
281 bilayer, embedded proteins, and attached organic molecules that collectively control the
282 selective permeability of ions, organic molecules, and particles across the cell boundary. The
283 intact plasma membrane, therefore, prevents the passage of many water-soluble mitochondrial
284 substrates, such as succinate or adenosine diphosphate (ADP), that are required for the analysis
285 of respiratory capacity at kinetically-saturating concentrations, thus limiting the scope of
286 investigations into mitochondrial respiratory function in intact cells. The cholesterol content of
287 the plasma membrane is high compared to mitochondrial membranes. Therefore, mild
288 detergents, such as digitonin and saponin, can be applied to selectively permeabilize the plasma
289 membrane by interaction with cholesterol and allow free exchange of cytosolic components
290 with ions and organic molecules of the immediate cell environment, while maintaining the
291 integrity and localization of organelles, cytoskeleton, and the nucleus. Application of optimum
292 concentrations of these mild detergents leads to the complete loss of cell viability, tested by
293 nuclear staining and washout of cytosolic marker enzymes such as lactate dehydrogenase, while
294 mitochondrial function remains intact, as shown by an unaltered respiration rate of isolated
295 mitochondria after the addition of such low concentrations of digitonin and saponin. In addition
296 to mechanical permeabilization during homogenization of fresh tissue, saponin may be applied
297 to ensure permeabilization of all cells. Crude homogenate and cells permeabilized in the
298 respiration chamber contain all components of the cell at highly diluted concentrations. All
299 mitochondria are retained in chemically-permeabilized mitochondrial preparations and crude
300 tissue homogenates. In the preparation of isolated mitochondria, the cells or tissues are
301 homogenized, and the mitochondria are separated from other cell fractions and purified by

302 differential centrifugation, entailing the loss of a significant fraction of mitochondria. The term
 303 mitochondrial preparation does not include further fractionation of mitochondrial components,
 304 as well as submitochondrial particles.

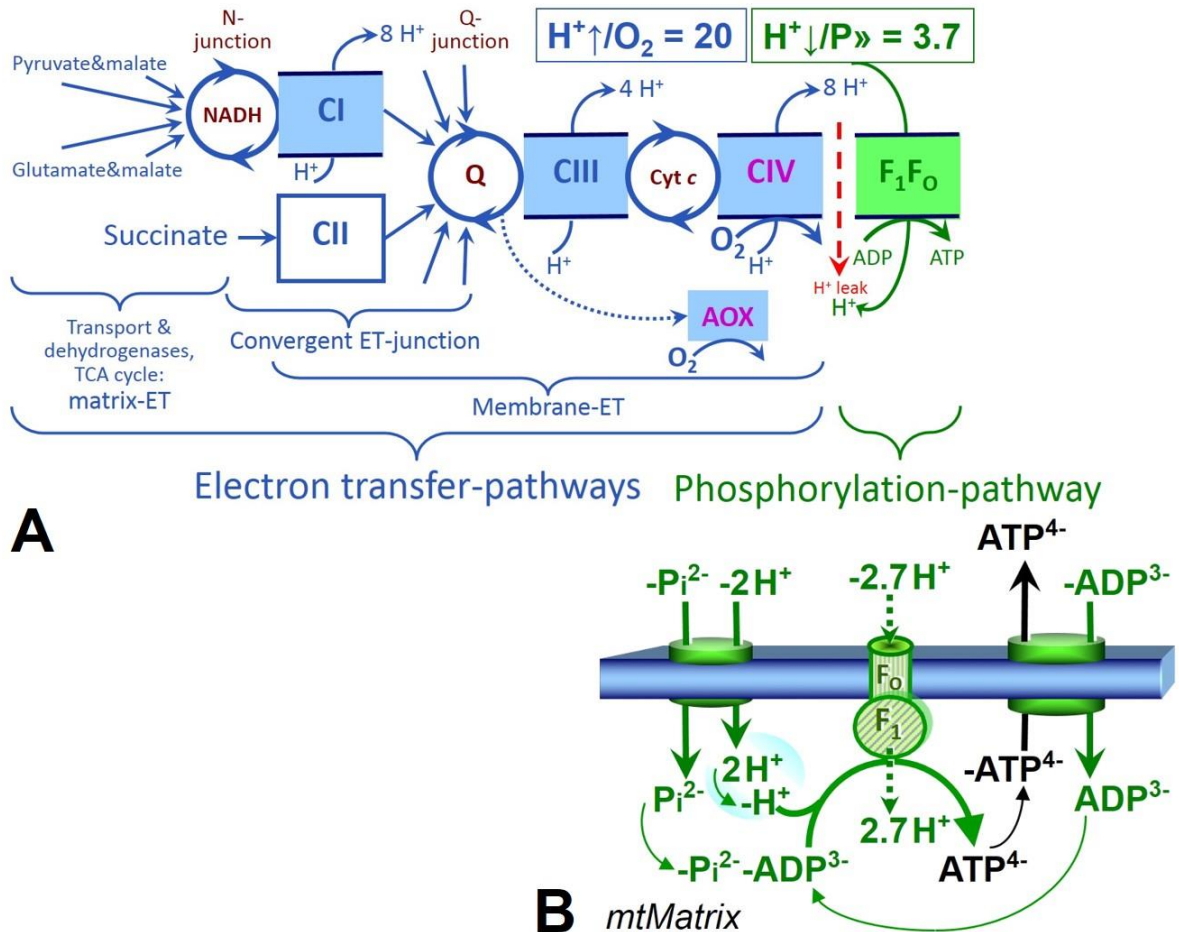
305
 306 *2.1. Three coupling states of mitochondrial preparations and residual oxygen consumption*

307 **Respiratory capacities in coupling control states:** To extend the classical nomenclature
 308 on mitochondrial coupling states (Section 2.4) by a concept-driven terminology that
 309 incorporates explicit information on the nature of the respiratory states, the terminology must
 310 be general and not restricted to any particular experimental protocol or mitochondrial
 311 preparation (Gnaiger 2009). We focus primarily on the conceptual ‘why’, along with
 312 clarification of the experimental ‘how’. In the following section, the concept-driven
 313 terminology is explained and coupling states are defined. We define respiratory capacities,
 314 comparable to channel capacity in information theory (Schneider 2006), as the upper bound of
 315 the rate of respiration measured in defined coupling control states and electron transfer-pathway
 316 (ET-pathway) control states. To provide a diagnostic reference for respiratory capacities of core
 317 energy metabolism, the capacity of *oxidative phosphorylation*, OXPHOS, is measured at
 318 kinetically-saturating concentrations of ADP and inorganic phosphate, P_i . The *oxidative* ET-
 319 capacity reveals the limitation of OXPHOS-capacity mediated by the *phosphorylation-*
 320 *pathway*. The ET- and phosphorylation-pathways comprise coupled segments of the OXPHOS-
 321 pathway. ET-capacity is measured as noncoupled respiration by application of *external*
 322 *uncouplers*. The contribution of *intrinsically uncoupled* oxygen consumption is most easily
 323 studied in the absence of ADP, *i.e.* by not stimulating phosphorylation, or by inhibition of the
 324 phosphorylation-pathway. The corresponding states are collectively classified as LEAK-states,
 325 when oxygen consumption compensates mainly for the proton leak (**Table 1**). Different
 326 coupling states are induced by: (1) adding ADP or P_i ; (2) inhibiting the phosphorylation-
 327 pathway; and (3) uncoupler titrations, while maintaining a defined ET-pathway state with
 328 constant fuel substrates and inhibitors of specific branches of the ET-pathway (**Fig. 1**).

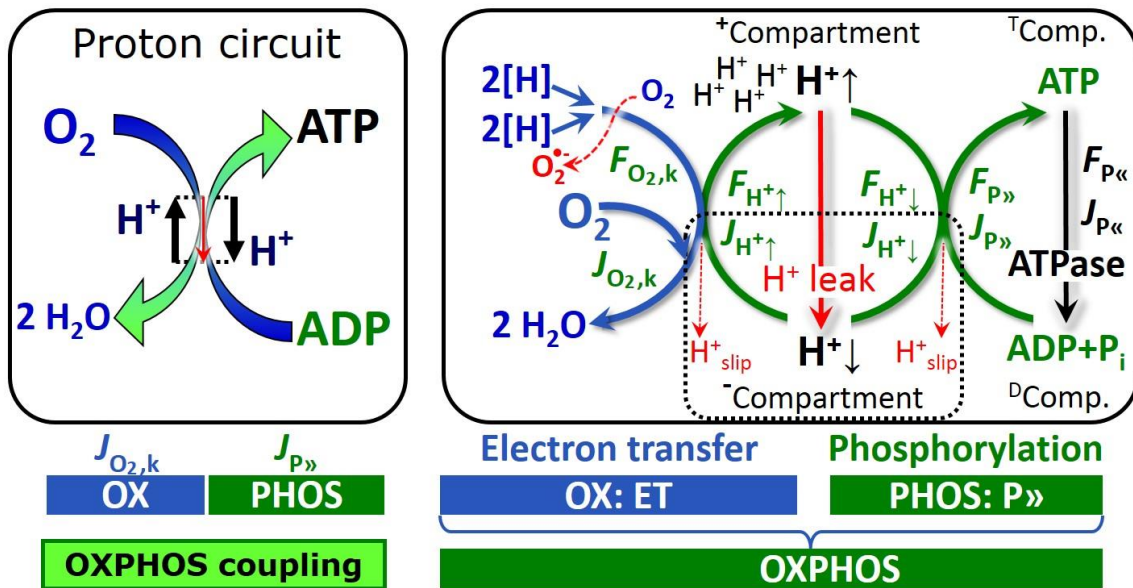
329 **Kinetic control:** Coupling control states are established in the study of mitochondrial
 330 preparations to obtain reference values for various output variables. Physiological conditions *in*
 331 *vivo* deviate from these experimentally obtained states. Since kinetically-saturating
 332 concentrations, *e.g.* of ADP or oxygen, may not apply to physiological intracellular conditions,
 333 relevant information is obtained in studies of kinetic responses to conditions intermediate
 334 between the LEAK state at zero [ADP] and the OXPHOS-state at saturating [ADP], or of
 335 respiratory capacities in the range between kinetically-saturating $[O_2]$ and anoxia (Gnaiger
 336 2001).

337 **Specification of dose of biochemical additions:** Nominal concentrations of substrates,
 338 uncouplers, inhibitors, and other biochemical reagents titrated to dissect mitochondrial function
 339 are usually reported as initial amount of substance concentration $[mol \cdot L^{-1}]$ in the incubation
 340 medium. When aiming at the measurement of kinetically saturated processes such as OXPHOS
 341 capacities, the concentrations for substrates can be chosen in light of the K_m' . In the case of
 342 hyperbolic kinetics, only 80% of maximum respiratory capacity is obtained at a substrate
 343 concentration of four times the K_m' , whereas substrate concentrations of 9, 19 and 49 times the
 344 K_m' are theoretically required for reaching 90%, 95% or 98% of the maximal rate (Gnaiger
 345 2001). Other reagents are chosen to inhibit or alter some process. The amount of these tools in
 346 an experimental incubation is selected to maximize effect, yet not lead to unacceptable off-
 347 target consequences that would adversely affect the data being sought. Specifying the amount
 348 of substance in an incubation as nominal concentration in the aqueous incubation medium can
 349 be ambiguous (Doskey *et al.* 2015), particularly when lipid-soluble substances (oligomycin;
 350 uncouplers) or cations (TPP+; fluorescent dyes such as safranin, TMRM) are applied which
 351 accumulate in biological membranes or in the mitochondrial matrix, respectively. For example,
 352 a dose of digitonin of $8 \text{ fmol} \cdot \text{cell}^{-1}$ ($10 \mu\text{g} \cdot 10^{-6} \text{ cells}$) is optimal for permeabilization of

353 endothelial cells, and the concentration in the incubation medium has to be adjusted according
 354 to the cell density applied (Pesta and Gnaiger 2012). Generally, dose/exposure can be specified
 355 per unit of biological sample, *i.e.* (nominal moles of xenobiotic)/(number of cells) [mol·cell⁻¹]
 356 or, as appropriate, per mass of biological sample [mol·g⁻¹]. This approach to specification of
 357 dose/exposure provides a scalable parameter that can be used to design experiments, help
 358 interpret a wide variety of experimental results, and provide absolute information that allows
 359 researchers worldwide to make the most use of published data (Doskey *et al.* 2015).
 360



361
 362 **Fig. 1. The oxidative phosphorylation-pathway, OXPHOS-pathway.** (A) Electron transfer,
 363 ET, coupled to phosphorylation. ET-pathways converge at the N- and Q-junction, as shown for
 364 the NADH- and succinate-pathway; additional arrows indicate electron entry into the Q-
 365 junction through electron transferring flavoprotein, glycerophosphate dehydrogenase, dihydro-
 366 orotate dehydrogenase, choline dehydrogenase, and sulfide-ubiquinone oxidoreductase. The
 367 branched pathway of oxygen consumption by alternative quinol oxidase (AOX) is indicated by
 368 the dotted arrow. The $H^+ \uparrow / O_2$ ratio is the outward proton flux from the matrix space divided by
 369 catabolic O_2 flux in the NADH-pathway. The $H^+ \downarrow / P \gg$ ratio is the inward proton flux from the
 370 inter-membrane space divided by the flux of phosphorylation of ADP to ATP. Due to proton
 371 leak and slip these are not fixed stoichiometries. (B) Phosphorylation-pathway catalyzed by the
 372 F_1F_0 ATP synthase, adenine nucleotide translocase, and inorganic phosphate transporter. The
 373 $H^+ \downarrow / P \gg$ stoichiometry is the sum of the coupling stoichiometry in the ATP synthase reaction
 374 ($-2.7 H^+$ from the intermembrane space, $2.7 H^+$ to the matrix) and the proton balance in the
 375 translocation of ADP^{2-} , ATP^{3-} and P_i^{2-} . See Eqs. 5 and 6 for further explanation. Modified from
 376 (A) Lemieux *et al.* (2017) and (B) Gnaiger (2014).



377
 378 **Fig. 2. The proton circuit and coupling in oxidative phosphorylation (OXPHOS).** Oxygen
 379 flux, $J_{O_2,k}$, through the catabolic ET-pathway k is coupled to flux through the phosphorylation-
 380 pathway of ADP to ATP, $J_{P\gg}$, by the proton pumps of the ET-pathway, driving the outward
 381 proton flux, $J_{H^+\uparrow}$, and generating the output protonmotive force, $F_{H^+\uparrow}$. ATP synthase is coupled
 382 to inward proton flux, $J_{H^+\downarrow}$, to phosphorylate ADP+ P_i to ATP, driven by the input protonmotive
 383 force, $F_{H^+\downarrow} = -F_{H^+\uparrow}$. $2[H]$ indicates the reduced hydrogen equivalents of fuel substrates that
 384 provide the chemical input force, $F_{O_2,k}$ [kJ/mol O_2], of the catabolic reaction k with oxygen
 385 (Gibbs energy of reaction per mole O_2 consumed in reaction k), typically in the range of -460
 386 to -480 kJ/mol. The output force is given by the phosphorylation potential difference (ADP
 387 phosphorylated to ATP), $F_{P\gg}$, which varies *in vivo* ranging from about 48 to 62 kJ/mol under
 388 physiological conditions (Gnaiger 1993a). Fluxes, J_B , and forces, F_B , are expressed in either
 389 chemical units, [$\text{mol}\cdot\text{s}^{-1}\cdot\text{m}^{-3}$] and [$\text{J}\cdot\text{mol}^{-1}$] respectively, or electrical units, [$\text{C}\cdot\text{s}^{-1}\cdot\text{m}^{-3}$] and [$\text{J}\cdot\text{C}^{-1}$]
 390 respectively. Fluxes are expressed per volume, V [m^3], of the system. The system defined by
 391 the boundaries (full black line) is not a black box, but is analysed as a compartmental system.
 392 The negative compartment ($^-\text{Compartment}$, enclosed by the dotted line) is the matrix space,
 393 separated from the positive compartment ($^+\text{Compartment}$) by the mtIM. ADP+ P_i and ATP are
 394 the substrate- and product-compartments (scalar ADP and ATP compartments, $^D\text{Comp.}$ and
 395 $^T\text{Comp.}$), respectively. Chemical potentials of all substrates and products involved in the scalar
 396 reactions are measured in the $^+\text{Compartment}$ for calculation of the scalar forces $F_{O_2,k}$ and $F_{P\gg} =$
 397 $-F_{P\ll}$ (**Box 2**). Modified from Gnaiger (2014).

398
 399 **Phosphorylation, $P\gg$:** *Phosphorylation* in the context of OXPBOS is defined as
 400 phosphorylation of ADP to ATP. On the other hand, the term phosphorylation is used generally
 401 in many different contexts, *e.g.* protein phosphorylation. This justifies consideration of a
 402 symbol more discriminating and specific than P as used in the P/O ratio (phosphate to atomic
 403 oxygen ratio; $O = 0.5 O_2$), where P indicates phosphorylation of ADP to ATP or GDP to GTP.
 404 We propose the symbol $P\gg$ for the endergonic direction of phosphorylation ADP \rightarrow ATP, and
 405 likewise the symbol $P\ll$ for the corresponding exergonic hydrolysis ATP \rightarrow ADP (**Fig. 2; Box**
 406 **3**). $J_{P\gg}/J_{O_2,k}$ ($P\gg/O_2$) is two times the ‘ P/O ’ ratio of classical bioenergetics. ATP synthase is the
 407 proton pump of the phosphorylation-pathway (**Fig. 1B**). $P\gg$ may also involve substrate-level
 408 phosphorylation as part of the tricarboxylic acid cycle (succinyl-CoA ligase) and
 409 phosphorylation of ADP catalyzed by phosphoenolpyruvate carboxykinase, adenylate kinase,
 410 creatine kinase, hexokinase and nucleoside diphosphate kinase (NDPK). Kinase cycles are
 411 involved in intracellular energy transfer and signal transduction for regulation of energy flux.

412 In isolated mammalian mitochondria ATP production catalyzed by adenylate kinase, $2\text{ADP} \leftrightarrow$
 413 $\text{ATP} + \text{AMP}$, proceeds without fuel substrates in the presence of ADP (Kömödi and Tretter
 414 2017). The effective P_{\gg}/O_2 ratio is diminished by: (1) the proton leak across the mtIM from low
 415 pH in the $^+$ Compartment to high pH in the $^-$ Compartment; (2) cycling of other cations; (3) proton
 416 slip in the proton pumps when a proton effectively is not pumped; and (4) electron leak in the
 417 univalent reduction of oxygen (O_2 ; dioxygen) to superoxide anion radical ($O_2^{\cdot -}$).
 418

419 **Table 1. Coupling states and residual oxygen consumption in mitochondrial**
 420 **preparations in relation to respiration- and phosphorylation-rate, $J_{O_2,k}$ and $J_{P_{\gg}}$,**
 421 **and protonmotive force, $F_{H^+\uparrow}$.** Coupling states are established at kinetically-
 422 saturating concentrations of fuel substrates and O_2 .

State	$J_{O_2,k}$	$J_{P_{\gg}}$	$F_{H^+\uparrow}$	Inducing factors	Limiting factors
LEAK	L ; low, proton leak-dependent respiration	0	max.	Proton leak, slip, and cation cycling	$J_{P_{\gg}} = 0$: (1) without ADP, L_N ; (2) max. ATP/ADP ratio, L_T ; or (3) inhibition of the phosphorylation-pathway, L_{Omy}
OXPHOS	P ; high, ADP-stimulated respiration	max.	high	Kinetically-saturating [ADP] and $[P_i]$	$J_{P_{\gg}}$ by phosphorylation-pathway; or $J_{O_2,k}$ by ET-capacity
ET	E ; max., noncoupled respiration	0	low	Optimal external uncoupler concentration for max. oxygen flux	$J_{O_2,k}$ by ET-capacity
ROX	R_{ox} ; min., residual O_2 consumption	0	0	$J_{O_2,Rox}$ in non-ET-pathway oxidation reactions	Full inhibition of ET-pathway; or absence of fuel substrates

423
 424 **LEAK-state (Fig. 3):** The
 425 LEAK-state is defined as a state
 426 of mitochondrial respiration
 427 when O_2 flux mainly
 428 compensates for the proton leak
 429 in the absence of ATP synthesis,
 430 at kinetically-saturating
 431 concentrations of O_2 and
 432 respiratory fuel substrates.
 433 LEAK-respiration is measured to
 434 obtain an indirect estimate of
 435 *intrinsic uncoupling* without
 436 addition of any experimental
 437 uncoupler: (1) in the absence of
 438 adenylates; (2) after depletion of
 439 ADP at maximum ATP/ADP
 440 ratio; or (3) after inhibition of the phosphorylation-pathway by inhibitors of ATP synthase, such as oligomycin, or adenine nucleotide translocase, such as carboxyatractyloside. It is important to consider adjustment of the nominal concentration of these inhibitors to the density of biological sample applied, to minimize or avoid inhibitory side-effects exerted on ET-capacity or even some uncoupling.
 441
 442
 443
 444

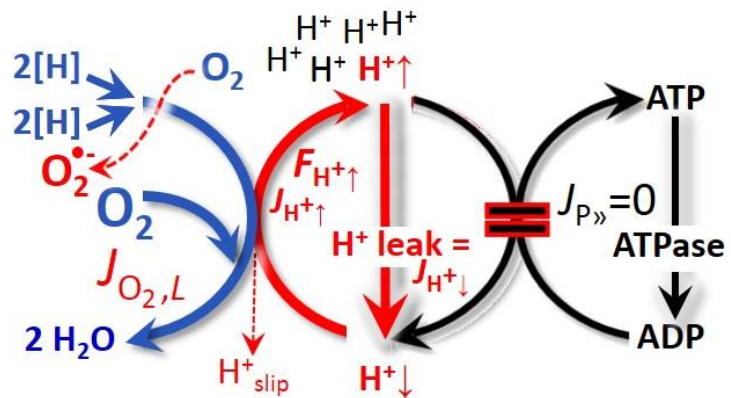


Fig. 3. LEAK-state: Phosphorylation is arrested, $J_{P_{\gg}} = 0$, and oxygen flux, $J_{O_2,L}$, is controlled mainly by the proton leak, $J_{H^+\downarrow,L}$, at maximum protonmotive force, $F_{H^+\uparrow}$. See also Fig. 2.

445 **Proton leak:** Proton leak is a leak current of protons. Proton leak is the *uncoupled* process
 446 in which protons diffuse across the mtIM in the dissipative direction of the downhill
 447 protonmotive force without coupling to phosphorylation (**Fig. 3**). The proton leak flux, $F_{H+\downarrow,L}$,
 448 depends non-linearly on the protonmotive force (Garlid *et al.* 1989; Divakaruni and Brand
 449 2011), is a property of the mtIM, may be enhanced due to possible contaminations by free fatty
 450 acids, and is physiologically controlled. In particular, inducible uncoupling mediated by
 451 uncoupling protein 1 (UCP1) is physiologically controlled, *e.g.*, in brown adipose tissue. UCP1
 452 is a proton channel of the mtIM facilitating the conductance of protons across the mtIM
 453 (Klingenberg 2017). As a consequence of this effective short-circuit, the protonmotive force
 454 diminishes, resulting in stimulation of electron transfer to oxygen and heat dissipation without
 455 phosphorylation of ADP. Mitochondrial injuries may lead to *dyscoupling* as a pathological or
 456 toxicological cause of *uncoupled* respiration, *e.g.*, as a consequence of opening the permeability
 457 transition pore. Dyscoupled respiration is distinguished from the experimentally induced
 458 *noncoupled* respiration in the ET-state. Under physiological conditions, the proton leak is the
 459 dominant contributor to the overall leak current (Dufour *et al.* 1996).

460
461

Table 2. Distinction of terms related to coupling.

Term	Respiration	P \gg /O ₂	Note
Fully coupled	$P - L$	max.	OXPPOS-capacity corrected for LEAK-respiration (Fig. 6)
Well-coupled	P	high	Phosphorylating respiration with an intrinsic LEAK component (Fig. 4)
Loosely coupled	up to E	low	Inducibly uncoupled by UCP1 or Ca ²⁺ cycling
Dyscoupled	P	low	Pathologically, toxicologically, environmentally increased uncoupling, mitochondrial dysfunction
Uncoupled and Decoupled	L	0	Non-phosphorylating intrinsic LEAK-respiration without added protonophore (Fig. 3)
Noncoupled	E	0	Non-phosphorylating respiration stimulated to maximum flux at optimum exogenous uncoupler concentration (Fig. 5)

462
463

Proton slip: Proton slip is the *decoupled* process in which protons are only partially translocated by a proton pump of the ET-pathways and slip back to the original compartment (Dufour *et al.* 1996). Proton slip can also happen in association with the ATP-synthase, in which case the proton slips downhill across the pump to the matrix without contributing to ATP synthesis. In each case, proton slip is a property of the proton pump and increases with the turnover rate of the pump.

469
470
471
472

Cation cycling: There can be other cation contributors to leak current including calcium and probably magnesium. Calcium current is balanced by mitochondrial Na/Ca exchange, which is balanced by Na/H exchange or K/H exchange. This is another effective uncoupling mechanism different from proton leak and slip.

473
474
475

Small differences of terms, *e.g.*, uncoupled, noncoupled, are easily overlooked and may be erroneously perceived as identical. Even with an attempt at rigorous definition, the common use of such terms may remain vague (**Table 2**).

476 **OXPHOS-state (Fig. 4):**

477 The OXPHOS-state is defined as
 478 the respiratory state with
 479 kinetically-saturating
 480 concentrations of O_2 , respiratory
 481 and phosphorylation substrates,
 482 and absence of exogenous
 483 uncoupler, which provides an
 484 estimate of the maximal
 485 respiratory capacity in the
 486 OXPHOS-state for any given ET-
 487 pathway state. Respiratory
 488 capacities at kinetically-saturating
 489 substrate concentrations provide
 490 reference values or upper limits of
 491 performance, aiming at the
 492 generation of data sets for comparative purposes. Physiological activities and effects of
 493 substrate kinetics can be evaluated relative to OXPHOS capacities.

494 As discussed previously, 0.2 mM ADP does not fully saturate flux in isolated
 495 mitochondria (Gnaiger 2001; Puchowicz *et al.* 2004); greater ADP concentration is required,
 496 particularly in permeabilized muscle fibres and cardiomyocytes, to overcome limitations by
 497 intracellular diffusion and by the reduced conductance of the mitochondrial outer membrane,
 498 mtOM (Jepihhina *et al.* 2011, Illaste *et al.* 2012, Simson *et al.* 2016), either through interaction
 499 with tubulin (Rostovtseva *et al.* 2008) or other intracellular structures (Birkedal *et al.* 2014). In
 500 permeabilized muscle fibre bundles of high respiratory capacity, the apparent K_m for ADP
 501 increases up to 0.5 mM (Saks *et al.* 1998), indicating that >90% saturation is reached only at
 502 >5 mM ADP. Similar ADP concentrations are also required for accurate determination of
 503 OXPHOS-capacity in human clinical cancer samples and permeabilized cells (Klepinin *et al.*
 504 2016; Koit *et al.* 2017). Whereas 2.5 to 5 mM ADP is sufficient to obtain the actual OXPHOS-
 505 capacity in many types of permeabilized tissue and cell preparations, experimental validation
 506 is required in each specific case.

507 **Electron transfer-state**

508 (Fig. 5): The ET-state is defined as

509 as the *noncoupled* state with
 510 kinetically-saturating
 511 concentrations of O_2 , respiratory
 512 substrate and optimum
 513 *exogenous* uncoupler
 514 concentration for maximum O_2
 515 flux, as an estimate of oxidative
 516 ET-capacity. Inhibition of
 517 respiration is observed at higher
 518 than optimum uncoupler
 519 concentrations. As a
 520 consequence of the nearly
 521 collapsed protonmotive force,
 522 the driving force is insufficient
 523 for phosphorylation, and $J_{P_{\gg}}$ = 0.

524 Besides the three fundamental coupling states of mitochondrial preparations, the
 525 following respiratory state also is relevant to assess respiratory function:

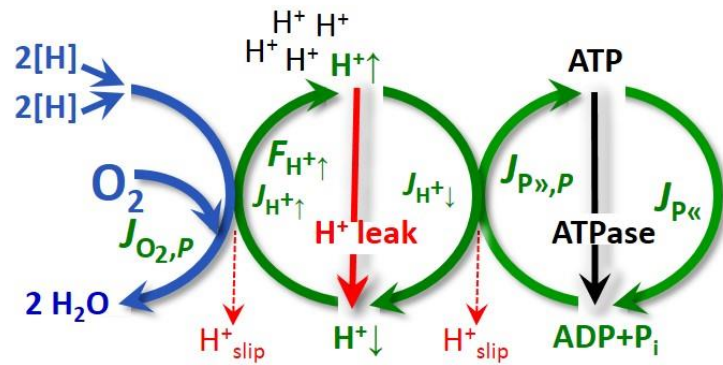


Fig. 4. OXPHOS-state: Phosphorylation, $J_{P_{\gg}}$, is stimulated by kinetically-saturating [ADP] and inorganic phosphate, $[P_i]$, and is supported by a high protonmotive force, $F_{H^+\uparrow}$. O_2 flux, $J_{O_2,P}$, is well-coupled at a P_{\gg}/O_2 ratio of $J_{P_{\gg},P}/J_{O_2,P}$. See also Fig. 2.

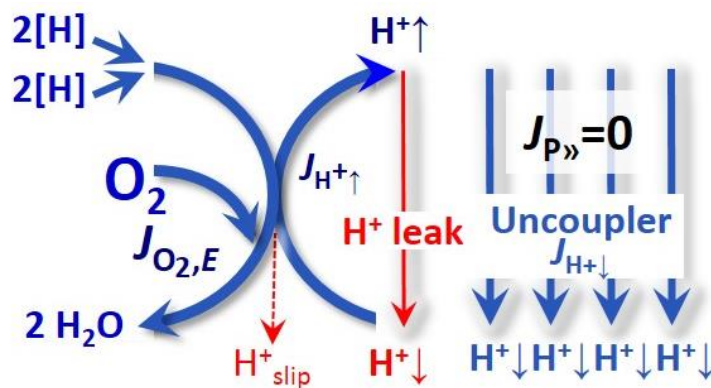


Fig. 5. ET-state: Noncoupled respiration, $J_{O_2,E}$, is maximum at optimum exogenous uncoupler concentration and phosphorylation is zero, $J_{P_{\gg}} = 0$. See also Fig. 2.

526 **ROX:** Residual oxygen consumption (ROX) is defined as O₂ consumption due to
 527 oxidative side reactions remaining after inhibition of ET with rotenone, malonic acid and
 528 antimycin A. Cyanide and azide not only inhibit CIV but several peroxidases which should be
 529 involved in ROX. ROX is not a coupling state but represents a baseline that is used to correct
 530 mitochondrial respiration in defined coupling states. ROX is not necessarily equivalent to non-
 531 mitochondrial respiration, considering oxygen-consuming reactions in mitochondria not related
 532 to ET, such as oxygen consumption in reactions catalyzed by monoamine oxidases (type A and
 533 B), monooxygenases (cytochrome P450 monooxygenases), dioxygenase (sulfur dioxygenase
 534 and trimethyllysine dioxygenase), several hydroxylases, and more. Mitochondrial preparations,
 535 especially those obtained from liver, may be contaminated by peroxisomes. This fact makes the
 536 exact determination of mitochondrial oxygen consumption and mitochondria-associated
 537 generation of reactive oxygen species complicated (Schönfeld *et al.* 2009). The dependence of
 538 ROX-linked oxygen consumption needs to be studied in detail with respect to non-ET enzyme
 539 activities, availability of specific substrates, oxygen concentration, and electron leakage leading
 540 to the formation of reactive oxygen species.

541

542 2.2. Coupling states and respiratory rates

543 It is important to distinguish metabolic *pathways* from metabolic *states* and the
 544 corresponding metabolic *rates*; for example: ET-pathways (Fig. 6), ET-state (Fig. 5), and ET-
 545 capacity, E , respectively (Table 1). The protonmotive force is *high* in the OXPHOS-state when
 546 it drives phosphorylation, *maximum* in the LEAK-state of coupled mitochondria, driven by
 547 LEAK-respiration at a minimum back flux of protons to the matrix side, and *very low* in the
 548 ET-state when uncouplers short-circuit the proton cycle (Table 1).

549

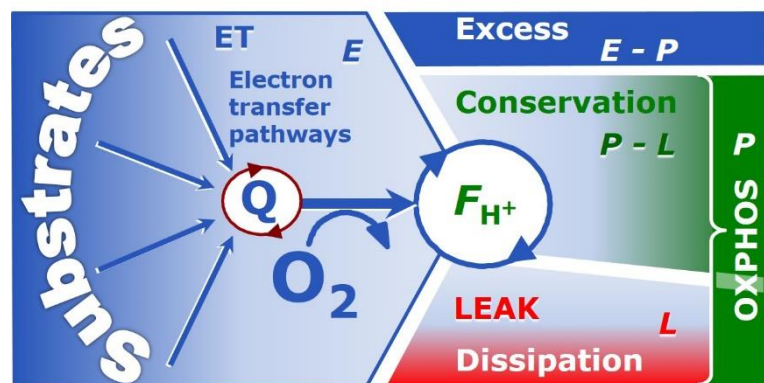
550 Fig. 6. Four-compartment model of oxidative phosphorylation.

551 Respiratory states (ET, OXPHOS, LEAK) and corresponding rates (E , P , L)
 552 are connected by the protonmotive force, F_{H^+} . Electron transfer-capacity, E , is
 553 partitioned into (1) dissipative LEAK-respiration, L , when the Gibbs energy change of catabolic
 554 O₂ consumption is irreversibly lost, (2) net OXPHOS-capacity, $P-L$, with partial conservation
 555 of the capacity to perform work, and (3) the excess capacity, $E-P$. Modified from Gnaiger
 556 (2014).

564

565 The three coupling states, ET, LEAK and OXPHOS, are shown schematically with the
 566 corresponding respiratory rates, abbreviated as E , L and P , respectively (Fig. 6). E may exceed
 567 or be equal to P , but E cannot theoretically be lower than P . $E < P$ must be discounted as an
 568 artefact, which may be caused experimentally by: (1) loss of oxidative capacity during the time
 569 course of the respirometric assay, since E is measured subsequently to P ; (2) using insufficient
 570 uncoupler concentrations; (3) using high uncoupler concentrations which inhibit ET (Gnaiger
 571 2008); (4) high oligomycin concentrations applied for measurement of L before titrations of
 572 uncoupler, when oligomycin exerts an inhibitory effect on E . On the other hand, the excess ET-
 573 capacity is overestimated if non-saturating [ADP] or [P_i] are used. See State 3 in the next
 574 section.

575 $E > P$ is observed in many types of mitochondria, varying between species, tissues and
 576 cell types. $E-P$ is the excess ET-capacity pushing the phosphorylation-flux (Fig. 1B) to the limit



577 of its *capacity of utilizing* the protonmotive force. Within any type of mitochondria, the
 578 magnitude of *E-P* depends on: (1) the pathway control state with single or multiple electron
 579 input into the Q-junction and involvement of three or fewer coupling sites determining the
 580 $H^+ \uparrow / O_2$ *coupling stoichiometry* (Fig. 1A); and (2) the *biochemical coupling efficiency* expressed
 581 as $(E-L)/E$, since an increase of *L* causes *P* to increase towards the limit of *E*. The *excess E-P*
 582 capacity, *E-P*, therefore, provides a sensitive diagnostic indicator of specific injuries of the
 583 phosphorylation-pathway, under conditions when *E* remains constant but *P* declines relative to
 584 controls (Fig. 6). Substrate cocktails supporting simultaneous convergent electron transfer to
 585 the Q-junction for reconstitution of tricarboxylic acid cycle (TCA cycle) function establish
 586 pathway control states with high ET-capacity, and consequently increase the sensitivity of the
 587 *E-P* assay.

588 When subtracting *L* from *P*, the dissipative LEAK component in the OXPHOS-state may
 589 be overestimated. This can be avoided by measuring LEAK-respiration in a state when the
 590 protonmotive force is adjusted to its slightly lower value in the OXPHOS-state, *e.g.*, by titration
 591 of an ET inhibitor (Divakaruni and Brand 2011). Any turnover-dependent components of
 592 proton leak and slip, however, are underestimated under these conditions (Garlid *et al.* 1993).
 593 In general, it is inappropriate to use the term *ATP production* or *ATP turnover* for the difference
 594 of oxygen consumption measured in states *P* and *L*. The difference *P-L* is the upper limit of the
 595 part of OXPHOS-capacity that is freely available for ATP production (corrected for LEAK-
 596 respiration) and is fully coupled to phosphorylation with a maximum mechanistic stoichiometry
 597 (Fig. 6).

598

599 2.3. Classical terminology for isolated mitochondria

600 *'When a code is familiar enough, it ceases appearing like a code; one forgets that*
 601 *there is a decoding mechanism. The message is identical with its meaning'*
 602 (Hofstadter 1979).

603 Chance and Williams (1955; 1956) introduced five classical states of mitochondrial respiration
 604 and cytochrome redox states. Table 3 shows a protocol with isolated mitochondria in a closed
 605 respirometric chamber, defining a sequence of respiratory states.

606

607

608

609

Table 3. Metabolic states of mitochondria (Chance and Williams, 1956; Table V).

State	[O ₂]	ADP level	Substrate Level	Respiration rate	Rate-limiting substance
1	>0	low	low	slow	ADP
2	>0	high	~0	slow	substrate
3	>0	high	high	fast	respiratory chain
4	>0	low	high	slow	ADP
5	0	high	high	0	oxygen

610

611 **State 1** is obtained after addition of isolated mitochondria to air-saturated
 612 isoosmotic/isotonic respiration medium containing inorganic phosphate, but no fuel substrates
 613 and no adenylates, *i.e.*, AMP, ADP, ATP.

614 **State 2** is induced by addition of a high concentration of ADP (typically 100 to 300 μ M),
 615 which stimulates respiration transiently on the basis of endogenous fuel substrates and
 616 phosphorylates only a small portion of the added ADP. State 2 is then obtained at a low
 617 respiratory activity limited by exhausted endogenous fuel substrate availability (Table 3). If
 618 addition of specific inhibitors of respiratory complexes, such as rotenone, does not cause a
 619 further decline of oxygen consumption, State 2 is equivalent to residual oxygen consumption

620 (See below.). If inhibition is observed, undefined endogenous fuel substrates are a confounding
 621 factor of pathway control, contributing to the effect of subsequently externally added substrates
 622 and inhibitors. In contrast to the original protocol, an alternative sequence of titration steps is
 623 frequently applied, in which the alternative ‘State 2’ has an entirely different meaning, when
 624 this second state is induced by addition of fuel substrate without ADP (LEAK-state; in contrast
 625 to State 2 defined in **Table 2** as a ROX state), followed by addition of ADP.

626 **State 3** is the state stimulated by addition of fuel substrates while the ADP concentration
 627 is still high (**Table 3**) and supports coupled energy transformation through oxidative
 628 phosphorylation. ‘High ADP’ is a concentration of ADP specifically selected to allow the
 629 measurement of State 3 to State 4 transitions of isolated mitochondria in a closed respirometric
 630 chamber. Repeated ADP titration re-establishes State 3 at ‘high ADP’. Starting at oxygen
 631 concentrations near air-saturation (ca. 200 μM O_2 at sea level and 37 $^\circ\text{C}$), the total ADP
 632 concentration added must be low enough (typically 100 to 300 μM) to allow phosphorylation
 633 to ATP at a coupled rate of oxygen consumption that does not lead to oxygen depletion during
 634 the transition to State 4. In contrast, kinetically-saturating ADP concentrations usually are an
 635 order of magnitude higher than ‘high ADP’, e.g. 2.5 mM in isolated mitochondria. The
 636 abbreviation State 3u is occasionally used in bioenergetics, to indicate the state of respiration
 637 after titration of an uncoupler, without sufficient emphasis on the fundamental difference
 638 between OXPHOS-capacity (*well-coupled* with an *endogenous* uncoupled component) and ET-
 639 capacity (*noncoupled*).

640 **State 4** is a LEAK-state that is obtained only if the mitochondrial preparation is intact
 641 and well-coupled. Depletion of ADP by phosphorylation to ATP leads to a decline in the rate
 642 of oxygen consumption in the transition from State 3 to State 4. Under these conditions, a
 643 maximum protonmotive force and high ATP/ADP ratio are maintained, and the $\text{P}\gg/\text{O}_2$ ratio can
 644 be calculated. State 4 respiration, L_T (**Table 1**), reflects intrinsic proton leak and intrinsic ATP
 645 hydrolysis activity. Oxygen consumption in State 4 is an overestimation of LEAK-respiration
 646 if the contaminating ATP hydrolysis activity recycles some ATP to ADP, $J_{P\ll}$, which stimulates
 647 respiration coupled to phosphorylation, $J_{P\gg} > 0$. This can be tested by inhibition of the
 648 phosphorylation-pathway using oligomycin, ensuring that $J_{P\gg} = 0$ (State 4o). Alternatively,
 649 sequential ADP titrations re-establish State 3, followed by State 3 to State 4 transitions while
 650 sufficient oxygen is available. However, anoxia may be reached before exhaustion of ADP
 651 (State 5).

652 **State 5** is the state after exhaustion of oxygen in a closed respirometric chamber.
 653 Diffusion of oxygen from the surroundings into the aqueous solution may be a confounding
 654 factor preventing complete anoxia (Gnaiger 2001). Chance and Williams (1955) provide an
 655 alternative definition of State 5, which gives it the meaning of ROX: ‘State 5 may be obtained
 656 by antimycin A treatment or by anaerobiosis’.

657 In **Table 3**, only States 3 and 4 (and ‘State 2’ in the alternative protocol without ADP;
 658 not included in the table) are coupling control states, with the restriction that O_2 flux in State 3
 659 may be limited kinetically by non-saturating ADP concentrations (**Table 1**).

660

661 **3. The protonmotive force and proton flux**

662 *3.1. Electric and chemical partial forces versus electrical and chemical units*

663 The protonmotive force across the mtIM (Mitchell 1961; Mitchell and Moyle 1967) was
 664 introduced most beautifully in the *Grey Book 1966* (Mitchell 2011),

$$665 \Delta p = \Delta \Psi + \Delta \mu_{\text{H}^+}/F \quad (\text{Eq. 1})$$

666 The protonmotive force, Δp , consists of two partial forces: (1) The electrical part, $\Delta \Psi$, is the
 667 difference of charge (electric potential difference), is not specific for H^+ , and can, therefore, be
 668 measured by the distribution of other permeable cations between the positive and negative
 669 compartment (**Fig. 2**). (2) The chemical part, $\Delta \mu_{\text{H}^+}$, is the chemical potential difference in H^+ ,
 670 is proportional to the pH difference, and incorporates the Faraday constant (**Table 4**).

671 **Faraday constant**, $F = eN_A$ [C/mol] (**Table 4**, note 1) enables the conversion between
 672 protonmotive force, $F_{H^+/e} \equiv \Delta p$ [J/C], expressed per *motive charge*, e [C], and protonmotive
 673 force, $F_{H^+/n} \equiv \Delta\tilde{\mu}_{H^+} = \Delta p \cdot F$ [J/mol], expressed per *motive amount of protons*, n [mol]. Proton
 674 charge, e , and amount of substance, n , are motive entities expressed in units C and mol,
 675 respectively. Taken together, F is the conversion factor for expressing protonmotive force and
 676 flux in motive units of e or n (Eq. 2; **Table 4**, Notes 1 and 2),

$$677 F_{H^+/n} = F_{H^+/e} \cdot e \cdot N_A \quad (\text{Eq. 2.1})$$

$$678 J_{H^+/n} = J_{H^+/e} / (e \cdot N_A) \quad (\text{Eq. 2.2})$$

679

680 **Table 4. Protonmotive force and flux matrix.** Columns: The protonmotive force is
 681 the sum of two *partial isomorphic forces*, F_{el} and $F_{H^+,d}$. Rows: Electrical and chemical
 682 formats (motive units, MU: C and mol, for e and n , respectively). The Faraday constant,
 683 F , converts protonmotive force and flux from format e to n . In contrast to force (state),
 684 the conjugated flux (rate) cannot be partitioned.
 685

State	Force		electric	+	chem.	Unit	Notes
Protonmotive force, e	Δp	=	$\Delta\psi$	+	$\Delta\mu_{H^+}/F$	$J \cdot C^{-1}$	1e
Chemiosmotic potential, n	$\Delta\tilde{\mu}_{H^+}$	=	$\Delta\psi \cdot F$	+	$\Delta\mu_{H^+}$	$J \cdot mol^{-1}$	1n
State	Isomorphic force		el	+	H⁺_d	$J \cdot MU^{-1}$	
Electric charge, e	$F_{H^+/e}$	=	$F_{el/e}$	+	$F_{H^+,d/e}$	$J \cdot C^{-1}$	2e
Amount of substance, n	$F_{H^+/n}$	=	$F_{el/n}$	+	$F_{H^+,d/n}$	$J \cdot mol^{-1}$	2n
Rate	Isomorphic flux		e	or	n	$MU \cdot s^{-1} \cdot m^{-3}$	
Electric charge, e	$J_{H^+/e}$		$J_{H^+/e}$			$C \cdot s^{-1} \cdot m^{-3}$	3e
Amount of substance, n	$J_{H^+/n}$				$J_{H^+/n}$	$mol \cdot s^{-1} \cdot m^{-3}$	3n

686

687 1: The Faraday constant, F , is the product of elementary charge ($e = 1.602\,176\,634 \cdot 10^{-19}$ C) and the
 688 Avogadro (Loschmidt) constant ($N_A = 6.022\,140\,76 \cdot 10^{23}$ mol⁻¹), $F = e \cdot N_A = 96,485.33$ C·mol⁻¹ (Gibney
 689 2017). F is the conversion factor between electrical and chemical units. $\Delta\tilde{\mu}_{H^+}$ is the chemiosmotic
 690 potential difference. 1e and 1n are the classical representations of 2e and 2n.

691 2: F_{H^+} is the protonmotive force expressed in formats e or n , expressed in units C or mol. $F_{el/e} \equiv \Delta\psi$ is
 692 the partial protonmotive force (el) acting generally on charged motive molecules (*i.e.* ions that are
 693 permeable across the mtIM). In contrast, $F_{H^+,d/n} \equiv \Delta\mu_{H^+}$ is the partial protonmotive force specific for
 694 proton diffusion, H⁺_d, irrespective of charge. The sign of the force is negative for exergonic
 695 transformations in which exergy is lost or dissipated, $F_{H^+,d}$, and positive for endergonic
 696 transformations which conserve exergy in a coupled exergonic process, $F_{H^+,d} = -F_{H^+,d}$ (**Box 3**).

697 3: The sign of the flux, J_{H^+} , depends on the definition of the compartmental direction of the translocation.
 698 For the outward direction, $J_{H^+,out}$, flux is positive since the direction involves formation of H⁺ in the
 699 *Compartment (H⁺_↑ is added, $v_{H^+,out} = 1$; and H⁺_↓ is removed, $v_{H^+,out} = -1$). Equally, $J_{H^+,in}$ is positive since
 700 the direction involves formation of H⁺ in the \bar{C} Compartment (H⁺_↓ is added, $v_{H^+,in} = 1$; and H⁺_↑ is
 701 removed, $v_{H^+,in} = -1$; **Fig. 2**). The product of flux and force is volume-specific power [$J \cdot s^{-1} \cdot m^{-3} = W \cdot m^{-3}$]:
 702 $P_{V,H^+} = J_{H^+,out/e} \cdot F_{H^+,out/e} = J_{H^+,out/n} \cdot F_{H^+,out/n}$.

703

704 In each format, the protonmotive force is expressed as the sum of two partial isomorphic
 705 forces. The complex symbols in Eq. 1 can be explained and visualized more explicitly by
 706 *partial isomorphic forces* as the components of the protonmotive force:

707 **Electric part of the protonmotive force:** (1) Isomorph e : $F_{el/e} \equiv \Delta\psi$ is the electric part
 708 of the protonmotive force expressed in electrical units joule per coulomb, *i.e.* volt [$V = J/C$].
 709 $F_{el/e}$ is defined as partial Gibbs energy change per *motive elementary charge*, e [C], not specific
 710 for proton charge (**Table 4**, Note 2e). (2) Isomorph n : $F_{el/n} \equiv \Delta\psi \cdot F$ is the electric force expressed
 711 in chemical units joule per mole [J/mol], defined as partial Gibbs energy change per *motive*
 712 *amount of charge*, n [mol], not specific for proton charge (**Table 4**, Note 2n).

713

714

Table 5. Power, exergy, force, flux, and advancement.

Expression	Symbol	Definition	Unit	Notes
Power, volume-specific	$P_{V, \text{tr}}$	$P_{V, \text{tr}} = J_{\text{tr}} \cdot F_{\text{tr}} = d_{\text{tr}} G \cdot dt^{-1}$	$\text{W} \cdot \text{m}^{-3} = \text{J} \cdot \text{s}^{-1} \cdot \text{m}^{-3}$	1
Force, isomorphic	F_{tr}	$F_{\text{tr}} = \partial G / \partial \xi_{\text{tr}}^{-1}$	$\text{J} \cdot \text{MU}^{-1}$	2
Flux, isomorphic	J_{tr}	$J_{\text{tr}} = d_{\text{tr}} \xi_{\text{tr}} \cdot dt^{-1} \cdot V^{-1}$	$\text{MU} \cdot \text{s}^{-1} \cdot \text{m}^{-3}$	3
Advancement, n	$d_{\text{tr}} \xi_{\text{H}^+/n}$	$d_{\text{tr}} \xi_{\text{H}^+/n} = d_{\text{tr}} n_{\text{H}^+} \cdot \nu_{\text{H}^+}^{-1}$	$\text{MU} = \text{mol}$	$4n$
Advancement, e	$d_{\text{tr}} \xi_{\text{H}^+/e}$	$d_{\text{tr}} \xi_{\text{H}^+/e} = d_{\text{tr}} e_{\text{H}^+} \cdot \nu_{\text{H}^+}^{-1}$	$\text{MU} = \text{C}$	$4e$
Electric partial force, e	$F_{e/e}$	$F_{e/e} \equiv \Delta \Psi = RT / (zF) \cdot \Delta \ln a_{Bz}$	$\text{V} = \text{J} \cdot \text{C}^{-1}$	$5e$
Electric partial force, n	$F_{e/n}$	$F_{e/n} \equiv \Delta \Psi \cdot zF = RT \cdot \Delta \ln a_{Bz}$	$\text{kJ} \cdot \text{mol}^{-1}$	$5n$
	at $z = 1$	$= 96.5 \cdot \Delta \Psi$	$\text{kJ} \cdot \text{mol}^{-1}$	
Chemical partial force, e	$F_{\text{H}^+, d/e}$	$F_{\text{H}^+, d/e} \equiv \Delta \mu_{\text{H}^+} / F = -RT / F \cdot \ln(10) \cdot \Delta \text{pH}$	$\text{J} \cdot \text{C}^{-1}$	$6e$
	at 37°C	$= -0.061 \cdot \Delta \text{pH}$	$\text{J} \cdot \text{C}^{-1}$	
Chemical partial force, n	$F_{\text{H}^+, d/n}$	$F_{\text{H}^+, d/n} \equiv \Delta \mu_{\text{H}^+} = -RT \cdot \ln(10) \cdot \Delta \text{pH}$	$\text{J} \cdot \text{mol}^{-1}$	$6n$
	at 37°C	$= -5.9 \cdot \Delta \text{pH}$	$\text{kJ} \cdot \text{mol}^{-1}$	

717

718 1 to 4: A motive entity, expressed in a motive unit [MU] is a characteristic for any type of transformation,
 719 tr. $\text{MU} = \text{mol}$ or C in the chemical or electrical format of proton translocation.

720 2: Isomorphic forces, F_{tr} , are related to the generalized forces, X_{tr} , of irreversible thermodynamics
 721 as $F_{\text{tr}} = -X_{\text{tr}} \cdot T$, and the force of chemical reactions is the negative affinity, $F_{\text{r}} = -A$ (Prigogine 1967).
 722 ∂G [J] is the partial Gibbs energy change in the advancement of transformation tr.

723 3: For $\text{MU} = \text{C}$, flow is electric current, I_{el} [$\text{A} = \text{C} \cdot \text{s}^{-1}$], vector flux is electric current density per area,
 724 \mathbf{J}_{el} , and compartmental flux is electric current density per volume, I_{el} [$\text{A} \cdot \text{m}^{-3}$], all expressed in
 725 electrical format.

726 $4n$: For a chemical reaction, the advancement of reaction r is $d_r \xi_B = d_r n_B \cdot \nu_B^{-1}$ [mol]. The stoichiometric
 727 number is $\nu_B = -1$ or $\nu_B = 1$, depending on B being a product or substrate, respectively, in reaction
 728 r involving one mole of B. The conjugated *intensive* molar quantity, $F_{B,r} = \partial G / \partial \xi_B$ [$\text{J} \cdot \text{mol}^{-1}$], is the
 729 chemical force of reaction or *reaction-motive* force per stoichiometric amount of B. In reaction
 730 kinetics, $d_r n_B$ is expressed as a volume-specific quantity, which is the partial contribution to the
 731 total concentration change of B, $d_r c_B = d_r n_B / V$ and $dc_B = dn_B / V$, respectively. In open systems with
 732 constant volume V , $dc_B = d_r c_B + d_e c_B$, where r indicates the *internal* reaction and e indicates the
 733 *external* flux of B into the unit volume of the system. At steady state the concentration does not
 734 change, $dc_B = 0$, when $d_r c_B$ is compensated for by the external flux of B, $d_r c_B = -d_e c_B$ (Gnaiger
 735 1993b). Alternatively, $dc_B = 0$ when B is held constant by different coupled reactions in which B
 736 acts as a substrate or a product.

737 $4e$: Scalar potential difference across the mitochondrial membrane. In a scalar electric transformation
 738 (flux of charge, *i.e.* volume-specific current, from the matrix space to the intermembrane and
 739 extramitochondrial space), the motive force is the difference of charge (**Box 2**). The endergonic
 740 direction of translocation is defined in **Fig. 2** as $\text{H}^+ \downarrow \rightarrow \text{H}^+ \uparrow$.

741 $5e$: $F = 96.5$ ($\text{kJ} \cdot \text{mol}^{-1}$) / V . z_B is the charge number of ion B. a_B is the (relative) activity of ion B, which
 742 in dilute solutions ($c < 0.1$ $\text{mol} \cdot \text{dm}^{-3}$) is approximately equal to c_B / c° , where c° is the standard
 743 concentration of 1 $\text{mol} \cdot \text{dm}^{-3}$. $\Delta \ln a_B = \ln a_2 - \ln a_1 = \ln(a_2 / a_1)$, when ion B diffuses or is translocated
 744 from compartment 1 to 2 (Eq. 4). Compartments 1 and 2 have to be defined in each case (**Fig.**
 745 **2**). Note that ion selective electrodes (pH or TPP^+ electrodes) respond to $\ln a_B$. $\Delta \ln a_{\text{H}^+} = -$
 746 $\ln(10) \cdot \Delta \text{pH}$.

- 747 6: $R = 8.31451 \text{ J}\cdot\text{mol}^{-1}\cdot\text{K}^{-1}$ is the gas constant. $RT = 2.479$ and $2.579 \text{ kJ}\cdot\text{mol}^{-1}$ at 298.15 and 310.15
 748 K (25 and $37 \text{ }^\circ\text{C}$), respectively. See Eq. 3 and 4.
 749 6e: $RT/F\cdot\Delta\ln a_{\text{H}^+}$ yields force in the electrical format [$\text{J}\cdot\text{C}^{-1} = \text{V}$]. $RT/F = 2.479$ and 2.579 mV at 298.15
 750 and 310.15 K , respectively, and $\ln(10)\cdot RT/F = 59.16$ and 61.54 mV , respectively.
 751 6n: $RT\cdot\Delta\ln a_{\text{H}^+}$ yields force in the chemical format [$\text{J}\cdot\text{mol}^{-1}$]. $\ln(10)\cdot RT = 5.708$ and $5.938 \text{ kJ}\cdot\text{mol}^{-1}$ at
 752 298.15 and 310.15 K , respectively.
 753

754 **Chemical part of the protonmotive force:** (1) Isomorph n : $F_{\text{H}^+,d/n} \equiv \Delta\mu_{\text{H}^+}$ is the chemical
 755 part (diffusion, displacement of H^+) of the protonmotive force expressed in units joule per mole
 756 [J/mol]. $F_{\text{H}^+,d/n}$ is defined as partial Gibbs energy change per *motive amount of protons*, n [mol]
 757 (**Table 4**, Note 2n). (2) Isomorph e : $F_{\text{H}^+,d/e} \equiv \Delta\mu_{\text{H}^+}/F$ is the chemical force expressed in units
 758 joule per coulomb [$\text{J}/\text{C} = \text{V}$], defined as partial Gibbs energy change per *motive amount of*
 759 *protons expressed in units of electric charge*, e [C], but specific for proton charge (**Table 4**,
 760 Note 2e).

761 Protonmotive means that there is a potential for the movement of protons, and force is a
 762 measure of the potential for motion. Motion is relative and not absolute (Principle of Galilean
 763 Relativity); likewise there is no absolute potential, but isomorphic forces are potential
 764 differences (**Table 5**, Notes 5 and 6),

$$765 F_{\text{el}/n} = \Delta\psi\cdot zF = RT\cdot\Delta\ln c_{\text{Bz}} \quad (\text{Eq. 3.1})$$

$$766 F_{\text{H}^+,d/n} = \Delta\mu_{\text{H}^+} = RT\cdot\Delta\ln c_{\text{H}^+} \quad (\text{Eq. 3.2})$$

767 The isomorphism of the electric and chemical partial forces is most clearly illustrated when
 768 expressing all terms (Eq. 3) as dimensionless quantities (Eq. 4). For diffusion of protons into
 769 the matrix space (**Fig. 2**),

$$770 F_{\text{el}/n}\cdot RT^{-1} = \ln(c_{\text{Bz}\uparrow}/c_{\text{Bz}\downarrow}) \quad (\text{Eq. 4.1})$$

$$771 F_{\text{H}^+,d/n}\cdot RT^{-1} = \ln(c_{\text{H}^+\uparrow}/c_{\text{H}^+\downarrow}) \quad (\text{Eq. 4.2})$$

772 An electric partial force of 0.2 V , expressed in the format of electric charge, $F_{\text{el}\uparrow/e}$ (**Table**
 773 **5**, Note 5e), can be expressed equivalently as $19 \text{ kJ}\cdot\text{mol}^{-1} \text{ H}^+\uparrow$, in the format of amount, $F_{\text{el}\uparrow/n}$
 774 (Note 5n). For a ΔpH of 1 unit, the chemical partial force in the format of amount, $F_{\text{H}^+\uparrow,d/n}$,
 775 changes by $5.9 \text{ kJ}\cdot\text{mol}^{-1}$ (**Table 5**, Note 6n), and chemical force in the format of charge, $F_{\text{H}^+\uparrow,d/e}$,
 776 changes by 0.06 V (Note 6e). Considering a driving force of $-470 \text{ kJ}\cdot\text{mol}^{-1} \text{ O}_2$ for oxidation, the
 777 thermodynamic limit of the $\text{H}^+\uparrow/\text{O}_2$ ratio is reached at a value of $470/19 = 24$, compared to a
 778 mechanistic stoichiometry of 20 (**Fig. 1**).
 779

780 3.2. Definitions

781 **Control and regulation:** The terms metabolic *control* and *regulation* are frequently used
 782 synonymously, but are distinguished in metabolic control analysis: ‘We could understand the
 783 regulation as the mechanism that occurs when a system maintains some variable constant over
 784 time, in spite of fluctuations in external conditions (homeostasis of the internal state). On the
 785 other hand, metabolic control is the power to change the state of the metabolism in response to
 786 an external signal’ (Fell 1997). Respiratory control may be induced by experimental control
 787 signals that *exert* an influence on: (1) ATP demand and ADP phosphorylation-rate; (2) fuel
 788 substrate composition, pathway competition; (3) available amounts of substrates and oxygen,
 789 *e.g.*, starvation and hypoxia; (3) the protonmotive force, redox states, flux-force relationships,
 790 coupling and efficiency; (4) Ca^{2+} and other ions including H^+ ; (5) inhibitors, *e.g.*, nitric oxide
 791 or intermediary metabolites, such as oxaloacetate; (6) signalling pathways and regulatory
 792 proteins, *e.g.* insulin resistance, transcription factor HIF-1 or inhibitory factor 1. *Mechanisms*
 793 of respiratory control and regulation include adjustments of: (1) enzyme activities by allosteric
 794 mechanisms and phosphorylation; (2) enzyme content, concentrations of cofactors and
 795 conserved moieties (such as adenylates, nicotinamide adenine dinucleotide [NAD^+/NADH],
 796 coenzyme Q, cytochrome *c*); (3) metabolic channeling by supercomplexes; and (4)
 797 mitochondrial density (enzyme concentrations and membrane area) and morphology (cristae
 798 folding, fission and fusion). (5) Mitochondria are targeted directly by hormones, thereby

799 affecting their energy metabolism (Lee *et al.* 2013; Gerö and Szabo 2016; Price and Dai 2016;
 800 Moreno *et al.* 2017). Evolutionary or acquired differences in the genetic and epigenetic basis
 801 of mitochondrial function (or dysfunction) between subjects and gene therapy; age; gender,
 802 biological sex, and hormone concentrations; life style including exercise and nutrition; and
 803 environmental issues including thermal, atmospheric, toxicological and pharmacological
 804 factors, exert an influence on all control mechanisms listed above. For reviews, see Brown
 805 1992; Gnaiger 1993a, 2009; 2014; Paradies *et al.* 2014; Morrow *et al.* 2017.

806 **Respiratory control and response:** Lack of control by a metabolic pathway, *e.g.*
 807 phosphorylation-pathway, does mean that there will be no response to a variable activating it,
 808 *e.g.* [ADP]. However, the reverse is not true as the absence of a response to [ADP] does not
 809 exclude the phosphorylation-pathway from having some degree of control. The degree of
 810 control of a component of the OXPHOS-pathway on an output variable, such as oxygen flux,
 811 will in general be different from the degree of control on other outputs, such as phosphorylation-
 812 flux or proton leak flux (**Box 2**). As such, it is necessary to be specific as to which input and
 813 output are under consideration (Fell 1997). Therefore, the term respiratory control is elaborated
 814 in more detail in the following section.

815 **Respiratory coupling control:** Respiratory control refers to the ability of mitochondria
 816 to adjust oxygen consumption in response to external control signals by engaging various
 817 mechanisms of control and regulation. Respiratory control is monitored in a mitochondrial
 818 preparation under conditions defined as respiratory states. When phosphorylation of ADP to
 819 ATP is stimulated or depressed, an increase or decrease is observed in electron flux linked to
 820 oxygen consumption in respiratory coupling states of intact mitochondria ('controlled states' in
 821 the classical terminology of bioenergetics). Alternatively, coupling of electron transfer with
 822 phosphorylation is disengaged by disruption of the integrity of the mtIM or by uncouplers,
 823 functioning like a clutch in a mechanical system. The corresponding coupling control state is
 824 characterized by high levels of oxygen consumption without control by phosphorylation
 825 ('uncontrolled state'). Energetic coupling is defined in **Box 4**. Loss of coupling lowers the
 826 efficiency by intrinsic uncoupling and decoupling, or pathological dyscoupling. Such
 827 generalized uncoupling is different from switching to mitochondrial pathways that involve
 828 fewer than three proton pumps ('coupling sites': Complexes CI, CIII and CIV), bypassing CI
 829 through multiple electron entries into the Q-junction (**Fig. 1**). A bypass of CIII and CIV is
 830 provided by alternative oxidases, which reduce oxygen without proton translocation.
 831 Reprogramming of mitochondrial pathways may be considered as a switch of gears (changing
 832 the stoichiometry) rather than uncoupling (loosening the stoichiometry).

833 **Pathway control states** are obtained in mitochondrial preparations by depletion of
 834 endogenous substrates and addition to the mitochondrial respiration medium of fuel substrates
 835 (CHNO) and specific inhibitors, activating selected mitochondrial pathways (**Fig. 1**). Coupling
 836 control states and pathway control states are complementary, since mitochondrial preparations
 837 depend on an exogenous supply of pathway-specific fuel substrates and oxygen (Gnaiger 2014).
 838

839 **Box 2: Metabolic fluxes and flows: vectorial and scalar**

840 In mitochondrial electron transfer (**Fig. 1**), vectorial transmembrane proton flux is coupled
 841 through the proton pumps CI, CIII and CIV to the catabolic flux of scalar reactions, collectively
 842 measured as oxygen flux. In **Fig. 2**, the scalar catabolic reaction, k , of oxygen consumption,
 843 $J_{O_2,k}$ [$\text{mol}\cdot\text{s}^{-1}\cdot\text{m}^{-3}$], is expressed as oxygen flux per volume, V [m^3], of the instrumental chamber
 844 (the system).

845 Fluxes are *vectors*, if they have *spatial* direction in addition to magnitude. A vector flux
 846 (surface-density of flow) is expressed per unit cross-sectional area, A [m^2], perpendicular to the
 847 direction of flux. If *flows*, I , are defined as extensive quantities of the *system*, as vector or scalar
 848 flow, I or I [$\text{mol}\cdot\text{s}^{-1}$], respectively, then the corresponding vector and scalar *fluxes*, J , are

849 obtained as $J = I \cdot A^{-1}$ [$\text{mol} \cdot \text{s}^{-1} \cdot \text{m}^{-2}$] and $J = I \cdot V^{-1}$ [$\text{mol} \cdot \text{s}^{-1} \cdot \text{m}^{-3}$], respectively, expressing flux as an
850 area-specific vector or volume-specific scalar quantity.

851 Vectorial transmembrane proton fluxes, $J_{\text{H}^+\uparrow}$ and $J_{\text{H}^+\downarrow}$, are analyzed in a heterogenous
852 compartmental system as a quantity with *directional* but not *spatial* information. Translocation
853 of protons across the mtIM has a defined direction, either from the negative compartment
854 (matrix space; negative or $\bar{\text{Compartment}}$) to the positive compartment (inter-membrane space;
855 positive or $^+\text{Compartment}$) or *vice versa* (**Fig. 2**). The arrows defining the direction of the
856 translocation between the two compartments may point upwards or downwards, right or left,
857 without any implication that these are actual directions in space. The $^+\text{Compartment}$ is neither
858 above nor below the $\bar{\text{Compartment}}$ in a spatial sense, but can be visualized arbitrarily in a figure
859 in the upper position (**Fig. 2**). In general, the *compartmental direction* of vectorial translocation
860 from the $\bar{\text{Compartment}}$ to the $^+\text{Compartment}$ is defined by assigning the initial and final state
861 as *ergodynamic compartments*, $\text{H}^+\downarrow \rightarrow \text{H}^+\uparrow$ or $0 = -\text{H}^+\downarrow + \text{H}^+\uparrow$, related to work (erg = work) that
862 must be performed to lift the proton from a lower to a higher electrochemical potential or from
863 the lower to the higher ergodynamic compartment (Gnaiger 1993b).

864 In direct analogy to *vectorial* translocation, the direction of a *scalar* chemical reaction, A
865 $\rightarrow B$ or $0 = -A + B$, is defined by assigning substrates and products, A and B, as ergodynamic
866 compartments. O_2 is defined as a substrate in respiratory O_2 consumption, which together with
867 the fuel substrates comprises the substrate compartment of the catabolic reaction (**Fig. 2**).
868 Volume-specific scalar O_2 flux is coupled (**Box 4**) to vectorial translocation. In order to
869 establish a quantitative relation between the coupled fluxes, both $J_{\text{O}_2, \text{k}}$ and $J_{\text{H}^+\uparrow}$ must be
870 expressed in identical units, [$\text{mol} \cdot \text{s}^{-1} \cdot \text{m}^{-3}$] or [$\text{C} \cdot \text{s}^{-1} \cdot \text{m}^{-3}$], yielding the $\text{H}^+\uparrow/\text{O}_2$ ratio (**Fig. 1**). The
871 *vectorial* proton flux in compartmental translocation has *compartmental direction*,
872 distinguished from a *vector* flux with *spatial direction*. Likewise, the corresponding
873 protonmotive force is defined as an electrochemical potential *difference* between two
874 compartments, in contrast to a *gradient* across the membrane or a vector force with defined
875 *spatial direction*.

876
877 **The steady-state:** Mitochondria represent a thermodynamically open system functioning
878 as a biochemical transformation system in non-equilibrium states. State variables (protonmotive
879 force; redox states) and metabolic fluxes (*rates*) are measured in defined mitochondrial
880 respiratory *states*. Strictly, steady states can be obtained only in open systems, in which changes
881 due to *internal* transformations, e.g., O_2 consumption, are instantaneously compensated for by
882 *external* fluxes e.g., O_2 supply, such that oxygen concentration does not change in the system
883 (Gnaiger 1993b). Mitochondrial respiratory states monitored in closed systems satisfy the
884 criteria of pseudo-steady states for limited periods of time, when changes in the system
885 (concentrations of O_2 , fuel substrates, ADP, P_i , H^+) do not exert significant effects on metabolic
886 fluxes (respiration, phosphorylation). Such pseudo-steady states require respiratory media with
887 sufficient buffering capacity and kinetically-saturating concentrations of substrates to be
888 maintained, and thus depend on the kinetics of the processes under investigation. Proton
889 turnover, $J_{\infty \text{H}^+}$, and ATP turnover, $J_{\infty \text{P}}$, proceed in the steady-state at constant $F_{\text{H}^+\uparrow}$, when $J_{\text{H}^+\infty}$
890 $= J_{\text{H}^+\uparrow} = J_{\text{H}^+\downarrow}$, and at constant $F_{\text{P}\gg}$, when $J_{\text{P}\infty} = J_{\text{P}\gg} = J_{\text{P}\ll}$ (**Fig. 2**).

891 3.3. Forces and fluxes in physics and thermodynamics

892 According to its definition in physics, a potential difference and as such the *protonmotive*
893 *force*, Δp , is not a force *per se* (Cohen *et al.* 2008). The fundamental forces of physics are
894 distinguished from *motive forces* of statistical and irreversible thermodynamics.
895 Complementary to the attempt towards unification of fundamental forces defined in physics,
896 the concepts of Nobel laureates Lars Onsager, Erwin Schrödinger, Ilya Prigogine and Peter
897 Mitchell unite (even if expressed in apparently unrelated terms) the diversity of *generalized* or
898 ‘isomorphic’ *flux-force* relationships, the product of which links to entropy production and the
899

900 Second Law of thermodynamics (Schrödinger 1944; Prigogine 1967). A *motive force* is the
 901 derivative of potentially available or ‘free’ energy (exergy) per *motive entity* (**Box 3**). Perhaps
 902 the first account of a *motive force* in energy transformation can be traced back to the Peripatetic
 903 school around 300 BC in the context of moving a lever, up to Newton’s motive force
 904 proportional to the alteration of motion (Coopersmith 2010). As a generalization, isomorphic
 905 motive forces are considered as *entropic forces* in physics (Wang 2010).

906

907 **Box 3: Endergonic and exergonic transformations, exergy and dissipation**

908 A chemical reaction, or any transformation, is exergonic if the Gibbs energy change (exergy)
 909 of the reaction is negative at constant temperature and pressure. The sum of Gibbs energy
 910 changes of all internal transformations in a system can only be negative, *i.e.* exergy is
 911 irreversibly dissipated. Endergonic reactions are characterized by positive Gibbs energies of
 912 reaction and cannot proceed spontaneously in the forward direction as defined. For instance,
 913 the endergonic reaction $P \gg$ is coupled to exergonic catabolic reactions, such that the total Gibbs
 914 energy change is negative, *i.e.* exergy must be dissipated for the reaction to proceed (**Fig. 2**).

915 In contrast, energy cannot be lost or produced in any internal process, which is the key
 916 message of the First Law of thermodynamics. Thus mitochondria are the sites of energy
 917 transformation but not energy production. Open and closed systems can gain energy and exergy
 918 only by external fluxes, *i.e.* uptake from the environment. Exergy is the potential to perform
 919 work. In the framework of flux-force relationships (**Box 4**), the *partial* derivative of Gibbs
 920 energy per advancement of a transformation is an isomorphic force, F_{tr} (**Table 5**, Note 2). In
 921 other words, force is equal to exergy per motive entity (in integral form, this definition takes
 922 care of non-isothermal processes). This formal generalization represents an appreciation of the
 923 conceptual beauty of Peter Mitchell’s innovation of the protonmotive force against the
 924 background of the established paradigm of the electromotive force (emf) defined at the limit of
 925 zero current (Cohen *et al.* 2008).

926

927 **Vectorial and scalar forces, and fluxes:** In chemical reactions and osmotic or diffusion
 928 processes occurring in a closed heterogeneous system, such as a chamber containing isolated
 929 mitochondria, scalar transformations occur without measured spatial direction but between
 930 separate compartments (displacement between the matrix and intermembrane space) or
 931 between energetically-separated chemical substances (reactions from substrates to products).
 932 Hence, the corresponding fluxes are not vectorial but scalar, and are expressed per volume and
 933 not per membrane area (**Box 2**). The corresponding motive forces are also scalar potential
 934 *differences* across the membrane (**Table 5**), without taking into account the *gradients* across
 935 the 6 nm thick mtIM (Rich 2003).

936 **Coupling:** In energetics (ergodynamics), coupling is defined as an energy transformation
 937 fuelled by an exergonic (downhill) input process driving the advancement of an endergonic
 938 (uphill) output process. The (negative) output/input power ratio is the efficiency of a coupled
 939 energy transformation (**Box 4**). At the limit of maximum efficiency of a completely coupled
 940 system, the (negative) input power equals the (positive) output power, such that the total power
 941 approaches zero at the maximum efficiency of 1, and the process becomes fully reversible
 942 without any dissipation of exergy, *i.e.* without entropy production.

943

944 **Box 4: Coupling, power and efficiency, at constant temperature and pressure**

945 Energetic coupling means that two processes of energy transformation are linked such that the
 946 input power, P_{in} , is the driving element of the output power, P_{out} , and the (negative) out/input
 947 power ratio is the efficiency. In general, power is work per unit time [$J \cdot s^{-1} = W$]. When
 948 describing a system with volume V without information on the internal structure, the output is
 949 defined as the *external work* (exergy) performed by the *total* system on its environment. Such
 950 a system may be open for any type of exchange, or closed and thus allowing only heat and work

951 to be exchanged across the system boundaries. This is the classical black box approach of
 952 thermodynamics. In contrast, in a colourful compartmental analysis of *internal* energy
 953 transformations (**Fig. 2**), the system is structured and described by definition of ergodynamic
 954 compartments (with information on the heterogeneity of the system; **Box 2**) and analysis of
 955 separate parts, *i.e.* a sequence of *partial* energy transformations, tr. At constant temperature and
 956 pressure, power per unit volume, $P_{V,tr} = P_{tr}/V$ [$\text{W}\cdot\text{m}^{-3}$], is the product of a volume-specific flux,
 957 J_{tr} , and its conjugated force, F_{tr} , and is directly linked to entropy production, $d_iS/dt = \sum_{tr} P_{tr}/T$
 958 [$\text{W}\cdot\text{K}^{-1}$], as generalized by irreversible thermodynamics (Prigogine 1967; Gnaiger 1993a,b).
 959 Output power of proton translocation and catabolic input power are (**Fig. 2**),

$$960 \quad \text{Output:} \quad P_{H^+\uparrow}/V = J_{H^+\uparrow} \cdot F_{H^+\uparrow}$$

$$961 \quad \text{Input:} \quad P_k/V = J_{O_2,k} \cdot F_{O_2,k}$$

962 $F_{O_2,k}$ is the exergonic input force with a negative sign, and, $F_{H^+\uparrow}$, is the endergonic output force
 963 with a positive sign (**Box 3**). Ergodynamic efficiency is the ratio of output/input power, or the
 964 flux ratio times force ratio (Gnaiger 1993a,b),

$$965 \quad \varepsilon = \frac{P_{H^+\uparrow}}{-P_k} = \frac{J_{H^+\uparrow}}{J_{O_2,k}} \cdot \frac{F_{H^+\uparrow}}{-F_{O_2,k}}$$

966 The concept of incomplete coupling relates exclusively to the first term, *i.e.* the flux ratio, or
 967 $H^+\uparrow/O_2$ ratio (**Fig. 1**). Likewise, respirometric definitions of the P_{\gg}/O_2 ratio and biochemical
 968 coupling efficiency (Section 3.2) consider flux ratios. In a completely coupled process, the
 969 power efficiency, ε , depends entirely on the force ratio, ranging from zero efficiency at an
 970 output force of zero, to the limiting output force and maximum efficiency of 1.0, when the total
 971 power of the coupled process, $P_t = P_k + P_{H^+\uparrow}$, equals zero, and any net flows are zero at
 972 ergodynamic equilibrium of a coupled process. Thermodynamic equilibrium is defined as the
 973 state when all potentials (all forces) are dissipated and equilibrate towards their minima of zero.
 974 In a fully or completely coupled process, output and input fluxes are directly proportional in a
 975 fixed ratio technically defined as a stoichiometric relationship (a gear ratio in a mechanical
 976 system). Such maximal stoichiometric output/input flux ratios are considered in OXPHOS
 977 analysis as the upper limits or mechanistic $H^+\uparrow/O_2$ and P_{\gg}/O_2 ratios (**Fig. 1**).

978
 979 **Coupled versus bound processes:** Since the chemiosmotic theory describes the
 980 mechanisms of coupling in OXPHOS, it may be interesting to ask if the electrical and chemical
 981 parts of proton translocation are coupled processes. This is not the case according to the
 982 definition of coupling. If the coupling mechanism is disengaged, the output process becomes
 983 independent of the input process, and both proceed in their downhill (exergonic) direction (**Fig.**
 984 **2**). It is not possible to physically uncouple the electrical and chemical processes, which are
 985 only *theoretically* partitioned as electrical and chemical components. The electrical and
 986 chemical partial protonmotive forces, $F_{el\uparrow}$ and $F_{H^+\uparrow,d}$, can be measured separately. In contrast,
 987 the corresponding proton flux, $J_{H^+\uparrow}$, is non-separable, *i.e.*, cannot be uncoupled. Then these are
 988 not *coupled* processes, but are defined as *bound* processes. The electrical and chemical parts
 989 are tightly bound partial forces, since the flux cannot be partitioned but expressed only in either
 990 an electrical or chemical format, $J_{H^+/e}$ or $J_{H^+/n}$ (**Table 4**).

991 992 **4. Normalization: fluxes and flows**

993 The challenges of measuring mitochondrial respiratory flux are matched by those of
 994 normalization, whereby O_2 consumption may be considered as the numerator and normalization
 995 as the complementary denominator, which are tightly linked in reporting the measurements in
 996 a format commensurate with the requirements of a database.

997 998 *4.1. Flux per chamber volume*

999 When the reactor volume does not change during the reaction, which is typical for liquid
 1000 phase reactions, the volume-specific flux of a chemical reaction r is the time derivative of the

1001 advancement of the reaction per unit volume, $J_{V,B} = d_r\zeta_B/dt \cdot V^{-1}$ [(mol·s⁻¹)·L⁻¹]. The *rate of*
 1002 *concentration change* is dc_B/dt [(mol·L⁻¹)·s⁻¹], where concentration is $c_B = n_B/V$. It is helpful to
 1003 make the subtle distinction between [mol·s⁻¹·L⁻¹] and [mol·L⁻¹·s⁻¹] for the fundamentally
 1004 different quantities of volume-specific flux and rate of concentration change, which merge to a
 1005 single expression only in closed systems. In open systems, external fluxes (such as O₂ supply)
 1006 are distinguished from internal transformations (metabolic flux, O₂ consumption). In a closed
 1007 system, external flows of all substances are zero and O₂ consumption (internal flow), I_{O_2}
 1008 [pmol·s⁻¹], causes a decline of the amount of O₂ in the system, n_{O_2} [nmol]. Normalization of
 1009 these quantities for the volume of the system, V [L = dm³], yields volume-specific O₂ flux, J_{V,O_2}
 1010 $= I_{O_2}/V$ [nmol·s⁻¹·L⁻¹], and O₂ concentration, [O₂] or $c_{O_2} = n_{O_2}/V$ [μmol·L⁻¹ = μM = nmol·mL⁻¹].
 1011 Instrumental background O₂ flux is due to external flux into a non-ideal closed respirometer,
 1012 such that total volume-specific flux has to be corrected for instrumental background O₂ flux,
 1013 *i.e.* O₂ diffusion into or out of the instrumental chamber. J_{V,O_2} is relevant mainly for
 1014 methodological reasons and should be compared with the accuracy of instrumental resolution
 1015 of background-corrected flux, *e.g.* ±1 nmol·s⁻¹·L⁻¹ (Gnaiger 2001). ‘Metabolic’ or catabolic
 1016 indicates O₂ flux, $J_{O_2,k}$, corrected for instrumental background O₂ flux and chemical background
 1017 O₂ flux due to autoxidation of chemical components added to the incubation medium.
 1018

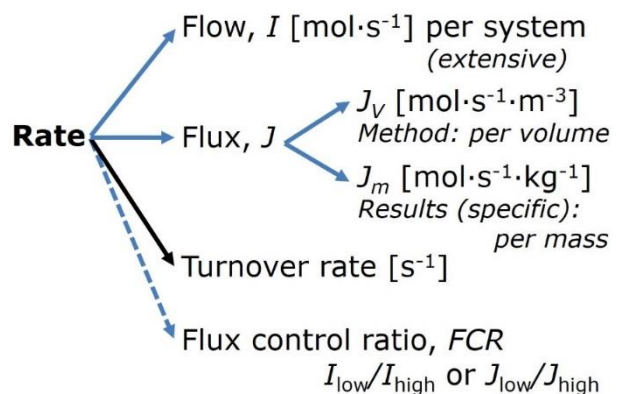
1019 4.2. System-specific and sample-specific normalization

1020 Application of common and generally defined units is required for direct transfer of
 1021 reported results into a database. The second [s] is the *SI* unit for the base quantity *time*. It is also
 1022 the standard time-unit used in solution chemical kinetics. **Table 6** lists some conversion factors
 1023 to obtain *SI* units. The term *rate* is not sufficiently defined to be useful for a database (**Fig. 7**).
 1024 The inconsistency of the meanings of rate becomes fully apparent when considering Galileo
 1025 Galilei’s famous principle, that ‘bodies of different weight all fall at the same rate (have a
 1026 constant acceleration)’ (Coopersmith 2010).

1027 **Extensive quantities:** An extensive quantity increases proportionally with system size.
 1028 The magnitude of an extensive quantity is completely additive for non-interacting subsystems,
 1029 such as mass or flow expressed per defined system. The magnitude of these quantities depends
 1030 on the extent or size of the system (Cohen *et al.* 2008).

1031 **Size-specific quantities:** ‘The adjective *specific* before the name of an extensive quantity
 1032 is often used to mean *divided by mass*’ (Cohen *et al.* 2008). Mass-specific flux is flow divided
 1033 by mass of the system. A mass-specific quantity is independent of the extent of non-interacting
 1034 homogenous subsystems. Tissue-specific quantities are of fundamental interest in comparative
 1035 mitochondrial physiology, where *specific* refers to the *type* rather than *mass* of the tissue. The
 1036 term *specific*, therefore, must be further clarified, such that tissue mass-specific, *e.g.*, muscle
 1037 mass-specific quantities are defined.
 1038

1039 **Fig. 7. Different meanings of rate may lead**
 1040 **to confusion, if the normalization is not**
 1041 **sufficiently specified.** Results are frequently
 1042 expressed as mass-specific *flux*, J_m , per mg
 1043 protein, dry or wet weight (mass). Cell
 1044 volume, V_{cell} , or mitochondrial volume, V_{mt} ,
 1045 may be used for normalization (volume-
 1046 specific flux, J_{Vcell} or J_{Vmt}), which then must
 1047 be clearly distinguished from flux, J_V ,
 1048 expressed for methodological reasons per
 1049 volume of the measurement system, or flow
 1050 per cell, I_X .
 1051



1052 **Molar quantities:** ‘The adjective *molar* before the name of an extensive quantity
 1053 generally means *divided by amount of substance*’ (Cohen *et al.* 2008). The notion that all molar
 1054 quantities then become *intensive* causes ambiguity in the meaning of *molar Gibbs energy*. It is
 1055 important to emphasize the fundamental difference between normalization for amount of
 1056 substance *in a system* or for amount of motive substance *in a transformation*. When the Gibbs
 1057 energy of a system, G [J], is divided by the amount of substance B in the system, n_B [mol], a
 1058 *size-specific* molar quantity is obtained, $G_B = G/n_B$ [J·mol⁻¹], which is not any force at all. In
 1059 contrast, when the partial Gibbs energy change, ∂G [J], is divided by the motive amount of
 1060 substance B in reaction r (advancement of reaction), $\partial_{r\zeta_B}$ [mol], the resulting intensive molar
 1061 quantity, $F_{B,r} = \partial G/\partial_{r\zeta_B}$ [J·mol⁻¹], is the chemical motive force of reaction r involving 1 mol B
 1062 (Table 5, Note 4).

1063 **Flow per system, I :** In analogy to electrical terms, flow as an extensive quantity (I ; per
 1064 system) is distinguished from flux as a size-specific quantity (J ; per system size) (Fig. 7).
 1065 Electric current is flow, I_{el} [A = C·s⁻¹] per system (extensive quantity). When dividing this
 1066 extensive quantity by system size (membrane area), a size-specific quantity is obtained, which
 1067 is electric flux (electric current density), J_{el} [A·m⁻² = C·s⁻¹·m⁻²].
 1068

1069 **Table 6. Sample concentrations and normalization of flux with SI base units.**

Expression	Symbol	Definition	SI Unit	Notes
Sample				
Identity of sample	X	Cells, animals, patients		
Number of sample entities X	N_X	Number of cells, <i>etc.</i>	x	
Mass of sample X	m_X		kg	1
Mass of entity X	M_X	$M_X = m_X \cdot N_X^{-1}$	kg·x ⁻¹	1
Mitochondria				
Mitochondria	mt	$X = mt$		
Amount of mt-elements	mte	Quantity of mt-marker	x_{mte}	
Concentrations				
Sample number concentration	C_{NX}	$C_{NX} = N_X \cdot V^{-1}$	x·m ⁻³	2
Sample mass concentration	C_{mX}	$C_{mX} = m_X \cdot V^{-1}$	kg·m ⁻³	
Mitochondrial concentration	C_{mte}	$C_{mte} = mte \cdot V^{-1}$	$x_{mte} \cdot m^{-3}$	3
Specific mitochondrial density	D_{mte}	$D_{mte} = mte \cdot m_X^{-1}$	$x_{mte} \cdot kg^{-1}$	4
Mitochondrial content, mte per entity X	mte_X	$mte_X = mte \cdot N_X^{-1}$	$x_{mte} \cdot x^{-1}$	5
O₂ flow and flux				
Flow	I_{O_2}	Internal flow	mol·s ⁻¹	6
Volume-specific flux	J_{V,O_2}	$J_{V,O_2} = I_{O_2} \cdot V^{-1}$	mol·s ⁻¹ ·m ⁻³	7
Flow per sample entity X	I_{X,O_2}	$I_{X,O_2} = J_{V,O_2} \cdot C_{NX}^{-1}$	mol·s ⁻¹ ·x ⁻¹	8
Mass-specific flux	J_{mX,O_2}	$J_{mX,O_2} = J_{V,O_2} \cdot C_{mX}^{-1}$	mol·s ⁻¹ ·kg ⁻¹	9
Mitochondria-specific flux	J_{mte,O_2}	$J_{mte,O_2} = J_{V,O_2} \cdot C_{mte}^{-1}$	mol·s ⁻¹ · x_{mte}^{-1}	10

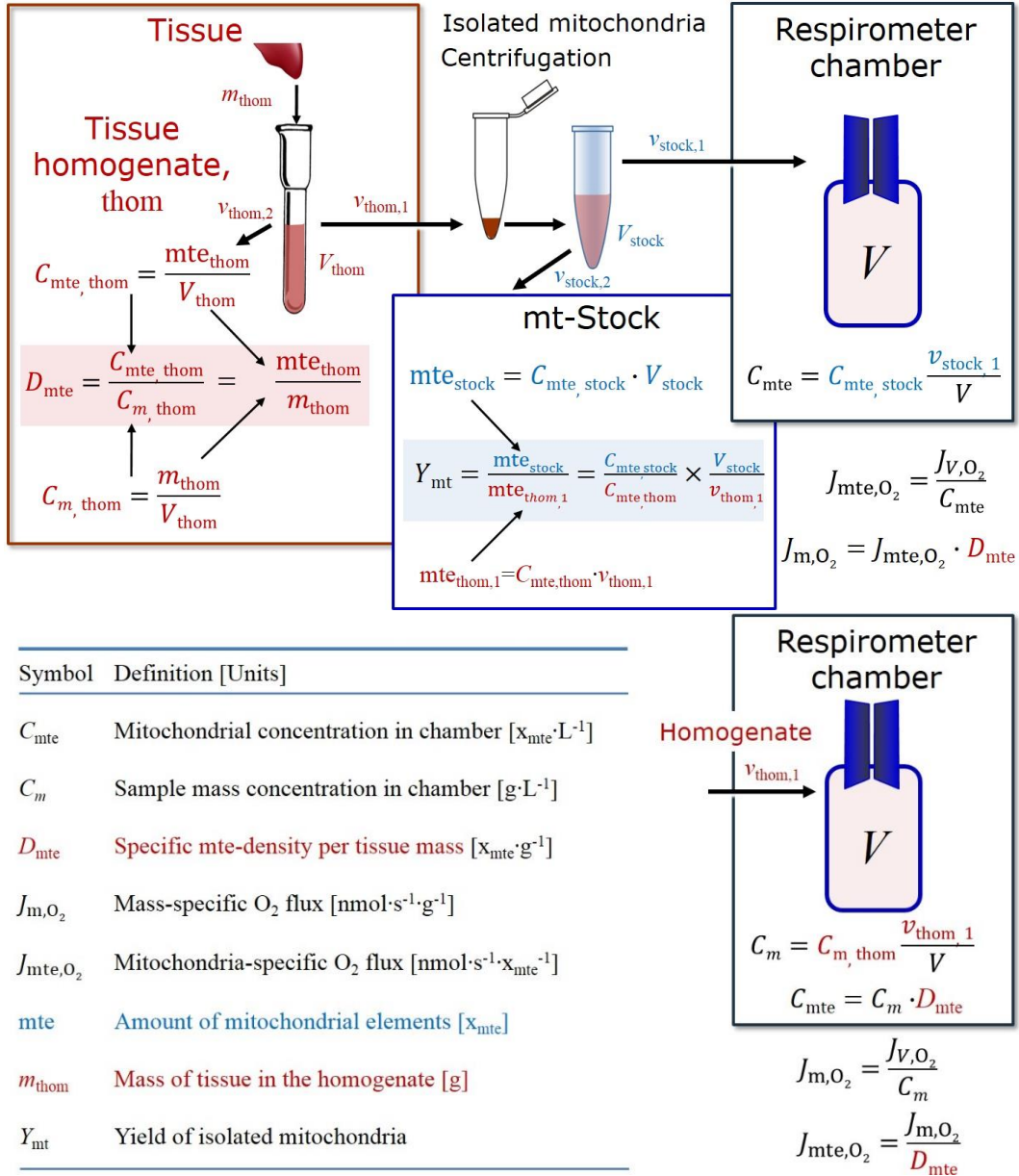
- 1071
 1072 1 The SI prefix k is used for the SI base unit of mass (kg = 1,000 g). In praxis, various SI prefixes are
 1073 used for convenience, to make numbers easily readable, e.g. 1 mg tissue, cell or mitochondrial mass
 1074 instead of 0.000001 kg.
 1075 2 In case $X = \text{cells}$, the sample number concentration is $C_{N_{cell}} = N_{cell} \cdot V^{-1}$, and volume may be expressed
 1076 in [dm³ = L] or [cm³ = mL]. See Table 7 for different sample types.
 1077 3 mt-concentration is an experimental variable, dependent on sample concentration: (1) $C_{mte} = mte \cdot V^{-1}$;
 1078 (2) $C_{mte} = mte_X \cdot C_{NX}$; (3) $C_{mte} = C_{mX} \cdot D_{mte}$.

- 1079 4 If the amount of mitochondria, m_{te} , is expressed as mitochondrial mass, then D_{mte} is the mass
 1080 fraction of mitochondria in the sample. If m_{te} is expressed as mitochondrial volume, V_{mt} , and the
 1081 mass of sample, m_X , is replaced by volume of sample, V_X , then D_{mte} is the volume fraction of
 1082 mitochondria in the sample.
- 1083 5 $m_{teX} = m_{te} \cdot N_X^{-1} = C_{mte} \cdot C_{NX}^{-1}$.
- 1084 6 O_2 can be replaced by other chemicals B to study different reactions, e.g. ATP, H_2O_2 , or
 1085 compartmental translocations, e.g. Ca^{2+} .
- 1086 7 I_{O_2} and V are defined per instrument chamber as a system of constant volume (and constant
 1087 temperature), which may be closed or open. I_{O_2} is abbreviated for $I_{O_2,r}$, i.e. the metabolic or internal
 1088 O_2 flow of the chemical reaction r in which O_2 is consumed, hence the negative stoichiometric
 1089 number, $\nu_{O_2} = -1$. $I_{O_2,r} = d_r n_{O_2} / dt \cdot \nu_{O_2}^{-1}$. If r includes all chemical reactions in which O_2 participates, then
 1090 $d_r n_{O_2} = dn_{O_2} - d_e n_{O_2}$, where dn_{O_2} is the change in the amount of O_2 in the instrument chamber and $d_e n_{O_2}$
 1091 is the amount of O_2 added externally to the system. At steady state, by definition $dn_{O_2} = 0$, hence $d_r n_{O_2}$
 1092 $= -d_e n_{O_2}$.
- 1093 8 J_{V,O_2} is an experimental variable, expressed per volume of the instrument chamber.
- 1094 9 I_{X,O_2} is a physiological variable, depending on the size of entity X .
- 1095 10 There are many ways to normalize for a mitochondrial marker, that are used in different experimental
 1096 approaches: (1) $J_{mte,O_2} = J_{V,O_2} \cdot C_{mte}^{-1}$; (2) $J_{mte,O_2} = J_{V,O_2} \cdot C_{mX}^{-1} \cdot D_{mte}^{-1} = J_{mX,O_2} \cdot D_{mte}^{-1}$; (3) $J_{mte,O_2} = J_{V,O_2} \cdot C_{NX}^{-1} \cdot m_{teX}^{-1}$
 1097 $= I_{X,O_2} \cdot m_{teX}^{-1}$; (4) $J_{mte,O_2} = I_{O_2} \cdot m_{te}^{-1}$.

1099 **Size-specific flux, J :** Metabolic O_2 flow per tissue increases as tissue mass is increased.
 1100 Tissue mass-specific O_2 flux should be independent of the size of the tissue sample studied in
 1101 the instrument chamber, but volume-specific O_2 flux (per volume of the instrument chamber,
 1102 V) should increase in direct proportion to the amount of sample in the chamber. Accurate
 1103 definition of the experimental system is decisive: whether the experimental chamber is the
 1104 closed, open, isothermal or non-isothermal *system* with defined volume as part of the
 1105 measurement apparatus, in contrast to the experimental *sample* in the chamber (**Table 6**).
 1106 Volume-specific O_2 flux depends on mass-concentration of the sample in the chamber, but
 1107 should be independent of the chamber volume. There are practical limitations to increasing the
 1108 mass-concentration of the sample in the chamber, when one is concerned about crowding
 1109 effects and instrumental time resolution.

1110 **Sample concentration C_{mX} :** Normalization for sample concentration is required for
 1111 reporting respiratory data. Consider a tissue or cells as the sample, X , and the sample mass, m_X
 1112 [mg] from which a mitochondrial preparation is obtained. m_X is frequently measured as wet or
 1113 dry weight, W_w or W_d [mg], or as amount of tissue or cell protein, $m_{Protein}$. In the case of
 1114 permeabilized tissues, cells, and homogenates, the sample concentration, $C_{mX} = m_X / V$ [$mg \cdot mL^{-1}$
 1115 $= g \cdot L^{-1}$], is simply the mass of the subsample of tissue that is transferred into the instrument
 1116 chamber. Part of the mitochondria from the tissue is lost during preparation of isolated
 1117 mitochondria. The fraction of mitochondria obtained is expressed as mitochondrial yield (**Fig.**
 1118 **8**). At a high mitochondrial yield the sample of isolated mitochondria is more representative of
 1119 the total mitochondrial population than in preparations characterized by low mitochondrial
 1120 yield. Determination of the mitochondrial yield is based on measurement of the concentration
 1121 of a mitochondrial marker in the tissue homogenate, $C_{mte,thom}$, which simultaneously provides
 1122 information on the specific mitochondrial density in the sample (**Fig. 8**).

1123 Tissues can contain multiple cell populations which may have distinct mitochondrial
 1124 subtypes. Mitochondria undergo dynamic fission and fusion cycles, and can exist in multiple
 1125 stages and sizes which may be altered by a range of factors. The isolation of mitochondria (often
 1126 achieved through differential centrifugation) can therefore yield a subsample of the
 1127 mitochondrial types present in a tissue, dependent on isolation protocols utilized (e.g.
 1128 centrifugation speed). This possible artefact should be taken into account when planning
 1129 experiments using isolated mitochondria. The tendency for mitochondria of specific sizes to be
 1130 enriched at different centrifugation speeds also has the potential to allow the isolation of specific
 1131 mitochondrial subpopulations and therefore the analysis of mitochondria from multiple cell
 1132 lineages within a single tissue.



1133

1134

1135

1136

1137

1138

1139

1140

1141

1142

1143

Fig. 8. Normalization of volume-specific flux of isolated mitochondria and tissue homogenate. A: Mitochondrial yield, Y_{mt} , in preparation of isolated mitochondria. $v_{thom,1}$ and $v_{stock,1}$ are the volumes transferred from the total volume, V_{thom} and V_{stock} , respectively. $mte_{thom,1}$ is the amount of mitochondrial elements in volume $v_{thom,1}$ used for isolation. **B:** In respirometry with homogenate, $v_{thom,1}$ is transferred directly into the respirometer chamber. See **Table 6** for further explanation of symbols.

Table 7. Some useful abbreviations of various sample types, X.

Identity of sample	X
Mitochondrial preparation	mtprep
Isolated mitochondria	imt
Tissue homogenate	thom
Permeabilized tissue	pti
Permeabilized fibre	pfi
Permeabilized cell	pce
Cell	ce
Organism	org

1144 **Mass-specific flux, J_{mX,O_2} :** Mass-specific flux is obtained by expressing respiration per
 1145 mass of sample, m_X [mg]. X is the type of sample, *e.g.*, tissue homogenate, permeabilized fibres
 1146 or cells. Volume-specific flux is divided by mass concentration of X , $J_{mX,O_2} = J_{V,O_2}/C_{mX}$; or flow
 1147 per cell is divided by mass per cell, $J_{m_{cell},O_2} = I_{cell,O_2}/M_{cell}$. If mass-specific O_2 flux is constant
 1148 and independent of sample size (expressed as mass), then there is no interaction between the
 1149 subsystems. A 1.5 mg and a 3.0 mg muscle sample respire at identical mass-specific flux.
 1150 Mass-specific O_2 flux, however, may change with the mass of a tissue sample, cells or isolated
 1151 mitochondria in the measuring chamber, in which case the nature of the interaction becomes an
 1152 issue. Optimization of cell density and arrangement is generally important and particularly in
 1153 experiments carried out in wells, considering the confluency of the cell monolayer or clumps
 1154 of cells (Salabei *et al.* 2014).

1155 **Number concentration, C_{NX} :** C_{NX} is the experimental *number concentration* of sample
 1156 in the case of cells or animals, *e.g.*, nematodes is $C_{NX} = N_X/V$ [$X \cdot L^{-1}$], where N_X is the number
 1157 of cells or organisms in the chamber (**Table 6**).

1158 **Flow per sample entity, I_{X,O_2} :** A special case of normalization is encountered in
 1159 respiratory studies with permeabilized (or intact) cells. If respiration is expressed per cell, the
 1160 O_2 flow per measurement system is replaced by the O_2 flow per cell, I_{cell,O_2} (**Table 6**). O_2 flow
 1161 can be calculated from volume-specific O_2 flux, J_{V,O_2} [$nmol \cdot s^{-1} \cdot L^{-1}$] (per V of the measurement
 1162 chamber [L]), divided by the number concentration of cells, $C_{N_{ce}} = N_{ce}/V$ [$cell \cdot L^{-1}$], where N_{ce}
 1163 is the number of cells in the chamber. Cellular O_2 flow can be compared between cells of
 1164 identical size. To take into account changes and differences in cell size, further normalization
 1165 is required to obtain cell size-specific or mitochondrial marker-specific O_2 flux (Renner *et al.*
 1166 2003).

1167 The complexity changes when the sample is a whole organism studied as an experimental
 1168 model. The well-established scaling law in respiratory physiology reveals a strong interaction
 1169 of O_2 consumption and individual body mass of an organism, since *basal* metabolic rate (flow)
 1170 does not increase linearly with body mass, whereas *maximum* mass-specific O_2 flux, \dot{V}_{O_2max} or
 1171 \dot{V}_{O_2peak} , is approximately constant across a large range of individual body mass (Weibel and
 1172 Hoppeler 2005), with individuals, breeds, and certain species deviating substantially from this
 1173 general relationship. \dot{V}_{O_2peak} of human endurance athletes is 60 to 80 mL $O_2 \cdot min^{-1} \cdot kg^{-1}$ body
 1174 mass, converted to J_{m,O_2peak} of 45 to 60 $nmol \cdot s^{-1} \cdot g^{-1}$ (Gnaiger 2014; **Table 8**).

1176 4.3. Normalization for mitochondrial content

1177 Normalization is a problematic subject and it is essential to consider the question of the
 1178 study. If the study aims to compare tissue performance, such as the effects of a certain treatment
 1179 on a specific tissue, then normalization can be successful, using tissue mass or protein content,
 1180 for example. If the aim, however, is to find differences of mitochondrial function independent
 1181 of mitochondrial density (**Table 6**), then normalization to a mitochondrial marker is imperative
 1182 (**Fig. 9**). However, one cannot assume that quantitative changes in various markers such as
 1183 mitochondrial proteins necessarily occur in parallel with one another. It is important to first
 1184 establish that the marker chosen is not selectively altered by the performed treatment. In
 1185 conclusion, the normalization must reflect the question under investigation to reach a satisfying
 1186 answer. On the other hand, the goal of comparing results across projects and institutions
 1187 requires some standardization on normalization for entry into a databank.

1188 **Mitochondrial concentration, C_{mte} , and mitochondrial markers:** It is important that
 1189 mitochondrial concentration in the tissue and the measurement chamber be quantified, as a
 1190 physiological output and result of mitochondrial biogenesis and degradation, and as a quantity
 1191 for normalization in functional analyses. Mitochondrial organelles comprise a dynamic cellular
 1192 reticulum in various states of fusion and fission. Hence the definition of an "amount" of
 1193 mitochondria is often misconceived: mitochondria cannot be counted as a number of occurring
 1194 elements. Therefore, quantification of the "amount" of mitochondria depends on measurement

1195 of chosen mitochondrial markers. ‘Mitochondria are the structural and functional elemental
 1196 units of cell respiration’ (Gnaiger 2014). The quantity of a mitochondrial marker can be
 1197 considered to reflect the amount of *elemental mitochondrial units* or *mitochondrial elements*,
 1198 mte. However, since mitochondrial quality changes under certain stimuli, particularly in
 1199 mitochondrial dysfunction and after exercise training (Pesta *et al.* 2011; Campos *et al.* 2017),
 1200 some markers can vary while other markers are unchanged: (1) Mitochondrial volume and
 1201 membrane area are structural markers, whereas mitochondrial protein mass is frequently used
 1202 as a marker for isolated mitochondria. (2) Molecular and enzymatic mitochondrial markers
 1203 (amounts or activities) can be selected as matrix markers, *e.g.*, citrate synthase activity, mtDNA;
 1204 mtIM-markers, *e.g.*, cytochrome *c* oxidase activity, *aa*₃ content, cardiolipin, or mtOM-markers,
 1205 *e.g.*, TOM20. (3) Extending the measurement of mitochondrial marker enzyme activity to
 1206 mitochondrial pathway capacity, measured as ET- or OXPHOS-capacity, can be considered as
 1207 an integrative functional mitochondrial marker.

1208 Depending on the type of mitochondrial marker, the mitochondrial elements, mte, are
 1209 expressed in marker-specific units. Although concentration and density are used synonymously
 1210 in physical chemistry, it is recommended to distinguish *experimental mitochondrial*
 1211 *concentration*, $C_{\text{mte}} = \text{mte}/V$ and *physiological mitochondrial density*, $D_{\text{mte}} = \text{mte}/m_X$. Then
 1212 mitochondrial density is the amount of mitochondrial elements per mass of tissue (Fig. 9). The
 1213 former is mitochondrial density multiplied by sample mass concentration, $C_{\text{mte}} = D_{\text{mte}} \cdot C_{mX}$, or
 1214 mitochondrial content multiplied by sample number concentration, $C_{\text{mte}} = \text{mte}_X \cdot C_{NX}$ (Table 6).
 1215

Flow, Performance	=	Element function	x	Element density	x	Size of entity
$\frac{\text{mol} \cdot \text{s}^{-1}}{X}$	=	$\frac{\text{mol} \cdot \text{s}^{-1}}{X_{\text{mte}}}$	·	$\frac{X_{\text{mte}}}{\text{kg}}$	·	$\frac{\text{kg}}{X}$

A	Flow	=	mt-specific flux	x	mt-structure, functional elements
	I_{X,O_2}	=	J_{mte,O_2}	·	mte_X
					$\frac{\text{mte}_X}{M_X} \cdot M_X$

I_{X,O_2}	=	J_{mte,O_2}	·	D_{mte}	·	M_X
$\frac{I_{X,O_2}}{M_X}$	=	$\frac{I_{X,O_2}}{\text{mte}_X}$	·	$\frac{\text{mte}_X}{M_X}$		

B	I_{X,O_2}	=	J_{mX,O_2}	·	M_X
	Flow	=	Entity mass- specific flux	x	Mass of entity

1216 **Fig. 9. Structure-function analysis of performance of an organism, organ or tissue,**
 1217 **or a cell (sample entity X). O₂ flow, I_{X,O_2} , is the product of performance per functional**
 1218 **element (element function, mitochondria-specific flux), element density**
 1219 **(mitochondrial density, D_{mte}), and size of entity X (mass M_X). (A) Structured analysis:**
 1220 **performance is the product of mitochondrial function (mt-specific flux) and structure**
 1221 **(functional elements; D_{mte} times mass of X). (B) Unstructured analysis: performance is**
 1222 **the product of entity mass-specific flux, $J_{mX,O_2} = I_{X,O_2}/M_X = I_{O_2}/m_X$ [$\text{mol} \cdot \text{s}^{-1} \cdot \text{kg}^{-1}$] and size of**
 1223 **entity, expressed as mass of X; $M_X = m_X \cdot N_X^{-1}$ [$\text{kg} \cdot \text{x}^{-1}$]. See Table 6 for further explanation**
 1224 **of quantities and units. Modified from Gnaiger (2014).**
 1225
 1226

1227 **Mitochondria-specific flux, $J_{\text{mte},\text{O}_2}$:** Volume-specific metabolic O_2 flux depends on: (1)
 1228 the sample concentration in the volume of the instrument chamber, C_{mX} , or C_{NX} ; (2) the
 1229 mitochondrial density in the sample, $D_{\text{mte}} = \text{mte}/m_X$ or $\text{mte}_X = \text{mte}/N_X$; and (3) the specific
 1230 mitochondrial activity or performance per elemental mitochondrial unit, $J_{\text{mte},\text{O}_2} = J_{V,\text{O}_2}/C_{\text{mte}}$
 1231 (Table 6). Obviously, the numerical results for $J_{\text{mte},\text{O}_2}$ vary according to the type of
 1232 mitochondrial marker chosen for measurement of mte and $C_{\text{mte}} = \text{mte}/V$.

1233

1234 4.4. Evaluation of mitochondrial markers

1235 Different methods are implicated in quantification of mitochondrial markers and have
 1236 different strengths. Some problems are common for all mitochondrial markers, mte: (1)
 1237 Accuracy of measurement is crucial, since even a highly accurate and reproducible
 1238 measurement of O_2 flux results in an inaccurate and noisy expression normalized for a biased
 1239 and noisy measurement of a mitochondrial marker. This problem is acute in mitochondrial
 1240 respiration because the denominators used (the mitochondrial markers) are often very small
 1241 moieties whose accurate and precise determination is difficult. This problem can be avoided
 1242 when O_2 fluxes measured in substrate-uncoupler-inhibitor titration protocols are normalized for
 1243 flux in a defined respiratory reference state, which is used as an *internal* marker and yields flux
 1244 control ratios, *FCRs* (Fig. 7). *FCRs* are independent of any *externally* measured markers and,
 1245 therefore, are statistically very robust, considering the limitations of ratios in general (Jasienski
 1246 and Bazzaz 1999). *FCRs* indicate qualitative changes of mitochondrial respiratory control, with
 1247 highest quantitative resolution, separating the effect of mitochondrial density or concentration
 1248 on J_{mX,O_2} and I_{X,O_2} from that of function per elemental mitochondrial marker, $J_{\text{mte},\text{O}_2}$ (Pesta *et al.*
 1249 2011; Gnaiger 2014). (2) If mitochondrial quality does not change and only the amount of
 1250 mitochondria varies as a determinant of mass-specific flux, any marker is equally qualified in
 1251 principle; then in practice selection of the optimum marker depends only on the accuracy and
 1252 precision of measurement of the mitochondrial marker. (3) If mitochondrial flux control ratios
 1253 change, then there may not be any best mitochondrial marker. In general, measurement of
 1254 multiple mitochondrial markers enables a comparison and evaluation of normalization for a
 1255 variety of mitochondrial markers. Particularly during postnatal development, the activity of
 1256 marker enzymes, such as cytochrome *c* oxidase and citrate synthase, follows different time
 1257 courses (Drahota *et al.* 2004). Evaluation of mitochondrial markers in healthy controls is
 1258 insufficient for providing guidelines for application in the diagnosis of pathological states and
 1259 specific treatments.

1260 In line with the concept of the respiratory control ratio (Chance and Williams 1955a), the
 1261 most readily used normalization is that of flux control ratios and flux control factors (Gnaiger
 1262 2014). Selection of the state of maximum flux in a protocol as the reference state has the
 1263 advantages of: (1) internal normalization; (2) statistical linearization of the response in the range
 1264 of 0 to 1; and (3) consideration of maximum flux for integrating a very large number of
 1265 elemental steps in the OXPHOS- or ET-pathways. This reduces the risk of selecting a functional
 1266 marker that is specifically altered by the treatment or pathodology, yet increases the chance that
 1267 the highly integrative pathway is disproportionately affected, *e.g.* the OXPHOS- rather than
 1268 ET-pathway in case of an enzymatic defect in the phosphorylation-pathway. In this case,
 1269 additional information can be obtained by reporting flux control ratios based on a reference
 1270 state which indicates stable tissue-mass specific flux. Stereological determination of
 1271 mitochondrial content via two-dimensional transmission electron microscopy can have
 1272 limitations due to the dynamics of mitochondrial size (Meinild Lundby *et al.* 2017). Accurate
 1273 determination of three-dimensional volume by two-dimensional microscopy can be both time
 1274 consuming and statistically challenging (Larsen *et al.* 2012). Using mitochondrial marker
 1275 enzymes (citrate synthase activity, Complex I–IV amount or activity) for normalization of flux
 1276 is limited in part by the same factors that apply to the use of flux control ratios. Strong
 1277 correlations between various mitochondrial markers and citrate synthase activity (Reichmann

1278 *et al.* 1985; Boushel *et al.* 2007; Mogensen *et al.* 2007) are expected in a specific tissue of
 1279 healthy subjects and in disease states not specifically targeting citrate synthase. Citrate synthase
 1280 activity is acutely modifiable by exercise (Tonkonogi *et al.* 1997; Leek *et al.* 2001). Evaluation
 1281 of mitochondrial markers related to a selected age and sex cohort cannot be extrapolated to
 1282 provide recommendations for normalization in respirometric diagnosis of disease, in different
 1283 states of development and ageing, different cell types, tissues, and species. mtDNA normalised
 1284 to nDNA via qPCR is correlated to functional mitochondrial markers including OXPHOS- and
 1285 ET-capacity in some cases (Puntschart *et al.* 1995; Wang *et al.* 1999; Menshikova *et al.* 2006;
 1286 Boushel *et al.* 2007), but lack of such correlations have been reported (Menshikova *et al.* 2005;
 1287 Schultz and Wiesner 2000; Pesta *et al.* 2011). Several studies indicate a strong correlation
 1288 between cardiolipin content and increase in mitochondrial functionality with exercise
 1289 (Menshikova *et al.* 2005; Menshikova *et al.* 2007; Larsen *et al.* 2012; Faber *et al.* 2014), but its
 1290 use as a general mitochondrial biomarker in disease remains questionable.

1291

1292 4.5. Conversion: units and normalization

1293 Many different units have been used to report the rate of oxygen consumption, OCR
 1294 (**Table 8**). SI base units provide the common reference for introducing the theoretical principles
 1295 (**Fig. 7**), and are used with appropriately chosen SI prefixes to express numerical data in the
 1296 most practical format, with an effort towards unification within specific areas of application
 1297 (**Table 9**). For studies of cells, we recommend that respiration be expressed, as far as possible,
 1298 as: (1) O₂ flux normalized for a mitochondrial marker, for separation of the effects of
 1299 mitochondrial quality and content on cell respiration (this includes FCRs as a normalization for
 1300 a functional mitochondrial marker); (2) O₂ flux in units of cell volume or mass, for comparison
 1301 of respiration of cells with different cell size (Renner *et al.* 2003) and with studies on tissue
 1302 preparations, and (3) O₂ flow in units of attomole (10⁻¹⁸ mol) of O₂ consumed in a second by
 1303 each cell [amol·s⁻¹·cell⁻¹], numerically equivalent to [pmol·s⁻¹·10⁻⁶ cells]. This convention
 1304 allows information to be easily used when designing experiments in which oxygen consumption
 1305 must be considered. For example, to estimate the volume-specific O₂ flux in an instrument
 1306 chamber that would be expected at a particular cell number concentration, one simply needs to
 1307 multiply the flow per cell by the number of cells per volume of interest. This provides the
 1308 amount of O₂ [mol] consumed per time [s⁻¹] per unit volume [L⁻¹]. At an O₂ flow of 100
 1309 amol·s⁻¹·cell⁻¹ and a cell density of 10⁹ cells·L⁻¹ (10⁶ cells·mL⁻¹), the volume-specific O₂ flux is
 1310 100 nmol·s⁻¹·L⁻¹ (100 pmol·s⁻¹·mL⁻¹).

1311 Although volume is expressed as m³ using the SI base unit, the litre [dm³] is the basic unit
 1312 of volume for concentration and is used for most solution chemical kinetics. If one multiplies
 1313 $J_{\text{cell},\text{O}_2}$ by $C_{N\text{cell}}$, then the result will not only be the amount of O₂ [mol] consumed per time [s⁻¹]
 1314 in one litre [L⁻¹], but also the change in the concentration of oxygen per second (for any volume
 1315 of an ideally closed system). This is ideal for kinetic modeling as it blends with chemical rate
 1316 equations where concentrations are typically expressed in mol·L⁻¹ (Wagner *et al.* 2011). In
 1317 studies of multinuclear cells, such as differentiated skeletal muscle cells, it is easy to determine
 1318 the number of nuclei but not the total number of cells. A generalized concept, therefore, is
 1319 obtained by substituting cells by nuclei as the sample entity. This does not hold, however, for
 1320 enucleated platelets.

1321

1322 4.5. Conversion: oxygen, proton and ATP flux

1323 $J_{\text{O}_2,k}$ is coupled in mitochondrial steady states to proton cycling, $J_{\text{H}^+\infty} = J_{\text{H}^+\uparrow} = J_{\text{H}^+\downarrow}$ (**Fig.**
 1324 **2**). $J_{\text{H}^+\uparrow/n}$ and $J_{\text{H}^+\downarrow/n}$ [nmol·s⁻¹·L⁻¹] are converted into electrical units, $J_{\text{H}^+\uparrow/e}$ [mC·s⁻¹·L⁻¹ = mA·L⁻¹]
 1325 = $J_{\text{H}^+\uparrow/n}$ [nmol·s⁻¹·L⁻¹]· F [C·mol⁻¹]·10⁻⁶ (**Table 4**). At a $J_{\text{H}^+\uparrow}/J_{\text{O}_2,k}$ ratio or H⁺↑/O₂ of 20 (H⁺↑/O =
 1326 10), a volume-specific O₂ flux of 100 nmol·s⁻¹·L⁻¹ would correspond to a proton flux of 2,000
 1327 nmol H⁺↑·s⁻¹·L⁻¹ or volume-specific current of 193 mA·L⁻¹.

1328

$$J_{V,H^{\uparrow}/e} [\text{mA}\cdot\text{L}^{-1}] = J_{V,H^{\uparrow}/n} \cdot F \cdot 10^{-6} [\text{nmol}\cdot\text{s}^{-1}\cdot\text{L}^{-1}\cdot\text{mC}\cdot\text{nmol}^{-1}] \quad (\text{Eq. 5.1})$$

$$J_{V,H^{\uparrow}/e} [\text{mA}\cdot\text{L}^{-1}] = J_{V,O_2} \cdot (\text{H}^{\uparrow}/\text{O}_2) \cdot F \cdot 10^{-6} [\text{mC}\cdot\text{s}^{-1}\cdot\text{L}^{-1} = \text{mA}\cdot\text{L}^{-1}] \quad (\text{Eq. 5.2})$$

ET-capacity in various human cell types including HEK 293, primary HUVEC and fibroblasts ranges from 50 to 180 $\text{amol}\cdot\text{s}^{-1}\cdot\text{cell}^{-1}$, measured in intact cells in the noncoupled state (see Gnaiger 2014). At 100 $\text{amol}\cdot\text{s}^{-1}\cdot\text{cell}^{-1}$ corrected for R_{ox} (corresponding to a catabolic power of $-48 \text{ pW}\cdot\text{cell}^{-1}$), the current across the mt-membranes, I_e , approximates 193 $\text{pA}\cdot\text{cell}^{-1}$ or 0.2 nA per cell. See Rich (2003) for an extension of quantitative bioenergetics from the molecular to the human scale, with a transmembrane proton flux equivalent to 520 A in an adult at a catabolic power of -110 W. Modelling approaches illustrate the link between protonmotive force and currents (Willis *et al.* 2016). For NADH- and succinate-linked respiration, the mechanistic P_{\gg}/O_2 ratio (referring to the full 4 electron reduction of O_2) is calculated at $20/3.7 = 5.4$ and $12/3.7 = 3.3$, respectively (Eq. 6). The classical P_{\gg}/O ratios (referring to the 2 electron reduction of $0.5 O_2$) are 2.7 and 1.6 (Watt *et al.* 2010), in direct agreement with the measured P_{\gg}/O ratio for succinate of 1.58 ± 0.02 (Gnaiger *et al.* 2000; for detailed reviews see Wikström and Hummer 2012; Sazanov 2015),

$$P_{\gg}/O_2 = (\text{H}^{\uparrow}/\text{O}_2)/(\text{H}^{\downarrow}/P_{\gg}) \quad (\text{Eq. 6})$$

In summary (Fig. 1),

$$J_{V,P_{\gg}} [\text{nmol}\cdot\text{s}^{-1}\cdot\text{L}^{-1}] = J_{V,O_2} \cdot (\text{H}^{\uparrow}/\text{O}_2)/(\text{H}^{\downarrow}/P_{\gg}) \quad (\text{Eq. 7.1})$$

$$J_{V,P_{\gg}} [\text{nmol}\cdot\text{s}^{-1}\cdot\text{L}^{-1}] = J_{V,O_2} \cdot (P_{\gg}/O_2) \quad (\text{Eq. 7.2})$$

We consider isolated mitochondria as powerhouses and proton pumps as molecular machines to relate experimental results to energy metabolism of the intact cell. The cellular P_{\gg}/O_2 based on oxidation of glycogen is increased by the glycolytic (fermentative) substrate-level phosphorylation of 3 P_{\gg}/Glyc , *i.e.*, 0.5 mol P_{\gg} for each mol O_2 consumed in the complete oxidation of a mol glycosyl unit (Glyc). Adding 0.5 to the mitochondrial P_{\gg}/O_2 ratio of 5.4 yields a bioenergetic cell physiological P_{\gg}/O_2 ratio close to 6. Two NADH equivalents are formed during glycolysis and transported from the cytosol into the mitochondrial matrix, either by the malate-aspartate shuttle or by the glycerophosphate shuttle resulting in different theoretical yield of ATP generated by mitochondria, the energetic cost of which potentially must be taken into account. Considering also substrate-level phosphorylation in the TCA cycle, this high P_{\gg}/O_2 ratio not only reflects proton translocation and OXPHOS studied in isolation, but integrates mitochondrial physiology with energy transformation in the living cell (Gnaiger 1993a).

1361

1362

1363

1364

1365

Table 8. Conversion of various units used in respirometry and ergometry. e is the number of electrons or reducing equivalents. z_B is the charge number of entity B.

1 Unit	x	Multiplication factor	SI-Unit	Note
$\text{ng}\cdot\text{atom O}\cdot\text{s}^{-1}$	(2 e)	0.5	$\text{nmol O}_2\cdot\text{s}^{-1}$	
$\text{ng}\cdot\text{atom O}\cdot\text{min}^{-1}$	(2 e)	8.33	$\text{pmol O}_2\cdot\text{s}^{-1}$	
$\text{natom O}\cdot\text{min}^{-1}$	(2 e)	8.33	$\text{pmol O}_2\cdot\text{s}^{-1}$	
$\text{nmol O}_2\cdot\text{min}^{-1}$	(4 e)	16.67	$\text{pmol O}_2\cdot\text{s}^{-1}$	
$\text{nmol O}_2\cdot\text{h}^{-1}$	(4 e)	0.2778	$\text{pmol O}_2\cdot\text{s}^{-1}$	
$\text{mL O}_2\cdot\text{min}^{-1}$ at STPD ^a		0.744	$\mu\text{mol O}_2\cdot\text{s}^{-1}$	1
$\text{W} = \text{J/s}$ at -470 kJ/mol O_2		-2.128	$\mu\text{mol O}_2\cdot\text{s}^{-1}$	
$\text{mA} = \text{mC}\cdot\text{s}^{-1}$	($z_{H^+} = 1$)	10.36	$\text{nmol H}^+\cdot\text{s}^{-1}$	2
$\text{mA} = \text{mC}\cdot\text{s}^{-1}$	($z_{O_2} = 4$)	2.59	$\text{nmol O}_2\cdot\text{s}^{-1}$	2
$\text{nmol H}^+\cdot\text{s}^{-1}$	($z_{H^+} = 1$)	0.09649	mA	3
$\text{nmol O}_2\cdot\text{s}^{-1}$	($z_{O_2} = 4$)	0.38594	mA	3

- 1366 1 At standard temperature and pressure dry (STPD: 0 °C = 273.15 K and 1 atm =
 1367 101.325 kPa = 760 mmHg), the molar volume of an ideal gas, V_m , and V_{m,O_2} is
 1368 22.414 and 22.392 L·mol⁻¹ respectively. Rounded to three decimal places, both
 1369 values yield the conversion factor of 0.744. For comparison at NTPD (20 °C),
 1370 V_{m,O_2} is 24.038 L·mol⁻¹. Note that the *SI* standard pressure is 100 kPa.
 1371 2 The multiplication factor is $10^6/(z_B \cdot F)$.
 1372 3 The multiplication factor is $z_B \cdot F/10^6$.
 1373
 1374

Table 9. Conversion of units with preservation of numerical values.

Name	Frequently used unit	Equivalent unit	Note
Volume-specific flux, J_{V,O_2}	pmol·s ⁻¹ ·mL ⁻¹ mmol·s ⁻¹ ·L ⁻¹	nmol·s ⁻¹ ·L ⁻¹ mol·s ⁻¹ ·m ⁻³	1
Cell-specific flow, I_{O_2}	pmol·s ⁻¹ ·10 ⁻⁶ cells pmol·s ⁻¹ ·10 ⁻⁹ cells	amol·s ⁻¹ ·cell ⁻¹ zmol·s ⁻¹ ·cell ⁻¹	2 3
Cell number concentration, C_{Nce}	10 ⁶ cells·mL ⁻¹	10 ⁹ cells·L ⁻¹	
Mitochondrial protein concentration, C_{mte}	0.1 mg·mL ⁻¹	0.1 g·L ⁻¹	
Mass-specific flux, J_{m,O_2}	pmol·s ⁻¹ ·mg ⁻¹	nmol·s ⁻¹ ·g ⁻¹	4
Catabolic power, $P_{O_2,k}$	μW·10 ⁻⁶ cells	pW·cell ⁻¹	1
Volume	1,000 L L mL μL fL	m ³ (1,000 kg) dm ³ (kg) cm ³ (g) mm ³ (mg) μm ³ (pg)	5
Amount of substance concentration	M = mol·L ⁻¹	mol·dm ⁻³	

- 1375
 1376 1 pmol: picomole = 10⁻¹² mol 4 nmol: nanomole = 10⁻⁹ mol
 1377 2 amol: attomole = 10⁻¹⁸ mol 5 fL: femtolitre = 10⁻¹⁵ L
 1378 3 zmol: zeptomole = 10⁻²¹ mol
 1379

5. Conclusions

MitoEAGLE can serve as a gateway to better diagnose mitochondrial respiratory defects linked to genetic variation, age-related health risks, sex-specific mitochondrial performance, lifestyle with its effects on degenerative diseases, and thermal and chemical environment. The present recommendations on coupling control states and rates, linked to the concept of the protonmotive force will be extended in a series of reports on pathway control of mitochondrial respiration, respiratory states in intact cells, and harmonization of experimental procedures.

Box 5: Mitochondrial and cell respiration

Mitochondrial and cell respiration is the process of highly exergonic and exothermic energy transformation in which scalar redox reactions are coupled to vectorial ion translocation across a semipermeable membrane, which separates the small volume of a bacterial cell or mitochondrion from the larger volume of its surroundings. The electrochemical exergy can be partially conserved in the phosphorylation of ADP to ATP or in ion pumping, or dissipated in an electrochemical short-circuit. Respiration is thus clearly distinguished from fermentation as the counterpart of cellular core energy metabolism. Respiration is separated in mitochondrial preparations from the partial contribution of fermentative pathways of the intact cell. According to this definition, residual oxygen consumption, as measured after inhibition of mitochondrial electron transfer, does not belong to the class of catabolic reactions and is, therefore, subtracted from total oxygen consumption to obtain baseline-corrected respiration.

1400
 1401 The optimal choice for expressing mitochondrial and cell respiration (**Box 5**) as O₂ flow
 1402 per biological system, and normalization for specific tissue-markers (volume, mass, protein)
 1403 and mitochondrial markers (volume, protein, content, mtDNA, activity of marker enzymes,
 1404 respiratory reference state) is guided by the scientific question under study. Interpretation of
 1405 the obtained data depends critically on appropriate normalization, and therefore reporting rates
 1406 merely as nmol·s⁻¹ is discouraged, since it restricts the analysis to intra-experimental
 1407 comparison of relative (qualitative) differences. Expressing O₂ consumption per cell may not
 1408 be possible when dealing with tissues. For studies with mitochondrial preparations, we
 1409 recommend that normalizations be provided as far as possible: (1) on a per cell basis as O₂ flow
 1410 (a biophysical normalization); (2) per g cell or tissue protein, or per cell or tissue mass as mass-
 1411 specific O₂ flux (a cellular normalization); and (3) per mitochondrial marker as mt-specific flux
 1412 (a mitochondrial normalization). With information on cell size and the use of multiple
 1413 normalizations, maximum potential information is available (Renner *et al.* 2003; Wagner *et al.*
 1414 2011; Gnaiger 2014). When using isolated mitochondria, mitochondrial protein is a frequently
 1415 applied mitochondrial marker, the use of which is basically restricted to isolated mitochondria.
 1416 Mitochondrial markers, such as citrate synthase activity as an enzymatic matrix marker, provide
 1417 a link to the tissue of origin on the basis of calculating the mitochondrial yield, *i.e.*, the fraction
 1418 of mitochondrial marker obtained from a unit mass of tissue.

1419
 1420 **Acknowledgements**

1421 We thank M. Beno for management assistance. Supported by COST Action CA15203 MitoEAGLE and K-Regio
 1422 project MitoFit (EG).

1423 **Competing financial interests:** E.G. is founder and CEO of Oroboros Instruments, Innsbruck, Austria.

1424

1425 **6. References**

- 1426 Altmann R (1894) Die Elementarorganismen und ihre Beziehungen zu den Zellen. Zweite vermehrte Auflage.
 1427 Verlag Von Veit & Comp, Leipzig:160 pp.
 1428 Beard DA (2005) A biophysical model of the mitochondrial respiratory system and oxidative phosphorylation.
 1429 PLoS Comput Biol 1(4):e36.
 1430 Benda C (1898) Über die Spermatogenese der Vertebraten und höherer Evertbraten II Theil: Die Histogenese
 1431 der Spermien. Arch Anat Physiol 73:393-8.
 1432 Birkedal R, Laasmaa M, Vendelin M (2014) The location of energetic compartments affects energetic
 1433 communication in cardiomyocytes. Front Physiol 5:376. doi: 10.3389/fphys.2014.00376. eCollection 2014.
 1434 Breton S, Beaupré HD, Stewart DT, Hoeh WR, Blier PU (2007) The unusual system of doubly uniparental
 1435 inheritance of mtDNA: isn't one enough? Trends Genet 23:465-74.
 1436 Brown GC (1992) Control of respiration and ATP synthesis in mammalian mitochondria and cells. Biochem J
 1437 284:1-13.
 1438 Campos JC, Queliconi BB, Bozi LHM, Bechara LRG, Dourado PMM, Andres AM, Jannig PR, Gomes KMS,
 1439 Zambelli VO, Rocha-Resende C, Guatimosim S, Brum PC, Mochly-Rosen D, Gottlieb RA, Kowaltowski AJ,
 1440 Ferreira JCB (2017) Exercise reestablishes autophagic flux and mitochondrial quality control in heart failure.
 1441 Autophagy 13:1304-317.
 1442 Chance B, Williams GR (1955a) Respiratory enzymes in oxidative phosphorylation. I. Kinetics of oxygen
 1443 utilization. J Biol Chem 217:383-93.
 1444 Chance B, Williams GR (1955b) Respiratory enzymes in oxidative phosphorylation: III. The steady state. J Biol
 1445 Chem 217:409-27.
 1446 Chance B, Williams GR (1955c) Respiratory enzymes in oxidative phosphorylation. IV. The respiratory chain. J
 1447 Biol Chem 217:429-38.
 1448 Chance B, Williams GR (1956) The respiratory chain and oxidative phosphorylation. Adv Enzymol Relat Subj
 1449 Biochem 17:65-134.
 1450 Cobb LJ, Lee C, Xiao J, Yen K, Wong RG, Nakamura HK, Mehta HH, Gao Q, Ashur C, Huffman DM, Wan J,
 1451 Muzumdar R, Barzilai N, Cohen P (2016) Naturally occurring mitochondrial-derived peptides are age-
 1452 dependent regulators of apoptosis, insulin sensitivity, and inflammatory markers. Aging (Albany NY) 8:796-
 1453 809.
 1454 Cohen ER, Cvitas T, Frey JG, Holmström B, Kuchitsu K, Marquardt R, Mills I, Pavese F, Quack M, Stohner J,
 1455 Strauss HL, Takami M, Thor HL (2008) Quantities, units and symbols in physical chemistry, IUPAC Green
 1456 Book, 3rd Edition, 2nd Printing, IUPAC & RSC Publishing, Cambridge.

- 1457 Cooper H, Hedges LV, Valentine JC, eds (2009) The handbook of research synthesis and meta-analysis. Russell
1458 Sage Foundation.
- 1459 Coopersmith J (2010) Energy, the subtle concept. The discovery of Feynman's blocks from Leibnitz to Einstein.
1460 Oxford University Press:400 pp.
- 1461 Cummins J (1998) Mitochondrial DNA in mammalian reproduction. *Rev Reprod* 3:172–82.
- 1462 Dai Q, Shah AA, Garde RV, Yonish BA, Zhang L, Medvitz NA, Miller SE, Hansen EL, Dunn CN, Price TM
1463 (2013) A truncated progesterone receptor (PR-M) localizes to the mitochondrion and controls cellular
1464 respiration. *Mol Endocrinol* 27:741-53.
- 1465 Divakaruni AS, Brand MD (2011) The regulation and physiology of mitochondrial proton leak. *Physiology*
1466 (Bethesda) 26:192-205.
- 1467 Doskey CM, van 't Erve TJ, Wagner BA, Buettner GR (2015) Moles of a substance per cell is a highly
1468 informative dosing metric in cell culture. *PLOS ONE* 10:e0132572.
- 1469 Drahota Z, Milerová M, Stieglarová A, Houstek J, Ostádal B (2004) Developmental changes of cytochrome *c*
1470 oxidase and citrate synthase in rat heart homogenate. *Physiol Res* 53:119-22.
- 1471 Duarte FV, Palmeira CM, Rolo AP (2014) The role of microRNAs in mitochondria: small players acting wide.
1472 *Genes (Basel)* 5:865-86.
- 1473 Dufour S, Rousse N, Canioni P, Diolez P (1996) Top-down control analysis of temperature effect on oxidative
1474 phosphorylation. *Biochem J* 314:743-51.
- 1475 Ernster L, Schatz G (1981) Mitochondria: a historical review. *J Cell Biol* 91:227s-55s.
- 1476 Estabrook RW (1967) Mitochondrial respiratory control and the polarographic measurement of ADP:O ratios.
1477 *Methods Enzymol* 10:41-7.
- 1478 Faber C, Zhu ZJ, Castellino S, Wagner DS, Brown RH, Peterson RA, Gates L, Barton J, Bickett M, Hagerty L,
1479 Kimbrough C, Sola M, Bailey D, Jordan H, Elangbam CS (2014) Cardiolipin profiles as a potential
1480 biomarker of mitochondrial health in diet-induced obese mice subjected to exercise, diet-restriction and
1481 ephedrine treatment. *J Appl Toxicol* 34:1122-9.
- 1482 Fell D (1997) Understanding the control of metabolism. Portland Press.
- 1483 Garlid KD, Beavis AD, Ratkje SK (1989) On the nature of ion leaks in energy-transducing membranes. *Biochim*
1484 *Biophys Acta* 976:109-20.
- 1485 Garlid KD, Semrad C, Zinchenko V. Does redox slip contribute significantly to mitochondrial respiration? In:
1486 Schuster S, Rigoulet M, Ouhabi R, Mazat J-P, eds (1993) Modern trends in biothermokinetics. Plenum Press,
1487 New York, London:287-93.
- 1488 Gerö D, Szabo C (2016) Glucocorticoids suppress mitochondrial oxidant production via upregulation of
1489 uncoupling protein 2 in hyperglycemic endothelial cells. *PLoS One* 11:e0154813.
- 1490 Gibney E (2017) New definitions of scientific units are on the horizon. *Nature* 550:312–13.
- 1491 Gnaiger E. Efficiency and power strategies under hypoxia. Is low efficiency at high glycolytic ATP production a
1492 paradox? In: *Surviving Hypoxia: Mechanisms of Control and Adaptation*. Hochachka PW, Lutz PL, Sick T,
1493 Rosenthal M, Van den Thillart G, eds (1993a) CRC Press, Boca Raton, Ann Arbor, London, Tokyo:77-109.
- 1494 Gnaiger E (1993b) Nonequilibrium thermodynamics of energy transformations. *Pure Appl Chem* 65:1983-2002.
- 1495 Gnaiger E (2001) Bioenergetics at low oxygen: dependence of respiration and phosphorylation on oxygen and
1496 adenosine diphosphate supply. *Respir Physiol* 128:277-97.
- 1497 Gnaiger E (2009) Capacity of oxidative phosphorylation in human skeletal muscle. New perspectives of
1498 mitochondrial physiology. *Int J Biochem Cell Biol* 41:1837-45.
- 1499 Gnaiger E (2014) Mitochondrial pathways and respiratory control. An introduction to OXPHOS analysis. 4th ed.
1500 *Mitochondr Physiol Network* 19.12. Oroboros MiPNet Publications, Innsbruck:80 pp.
- 1501 Gnaiger E, Méndez G, Hand SC (2000) High phosphorylation efficiency and depression of uncoupled respiration
1502 in mitochondria under hypoxia. *Proc Natl Acad Sci USA* 97:11080-5.
- 1503 Greggio C, Jha P, Kulkarni SS, Lagarrigue S, Broskey NT, Boutant M, Wang X, Conde Alonso S, Ofori E,
1504 Auwerx J, Cantó C, Amati F (2017) Enhanced respiratory chain supercomplex formation in response to
1505 exercise in human skeletal muscle. *Cell Metab* 25:301-11.
- 1506 Hofstadter DR (1979) Gödel, Escher, Bach: An eternal golden braid. A metaphorical fugue on minds and
1507 machines in the spirit of Lewis Carroll. Harvester Press:499 pp.
- 1508 Illaste A, Laasmaa M, Peterson P, Vendelin M (2012) Analysis of molecular movement reveals latticelike
1509 obstructions to diffusion in heart muscle cells. *Biophys J* 102:739-48.
- 1510 Jasienski M, Bazzaz FA (1999) The fallacy of ratios and the testability of models in biology. *Oikos* 84:321-26.
- 1511 Jepihhina N, Beraud N, Sepp M, Birkedal R, Vendelin M (2011) Permeabilized rat cardiomyocyte response
1512 demonstrates intracellular origin of diffusion obstacles. *Biophys J* 101:2112-21.
- 1513 Klepinin A, Ounpuu L, Guzun R, Chekulayev V, Timohhina N, Tepp K, Shevchuk I, Schlattner U, Kaambre T
1514 (2016) Simple oxygraphic analysis for the presence of adenylate kinase 1 and 2 in normal and tumor cells. *J*
1515 *Bioenerg Biomembr* 48:531-48.
- 1516 Klingenberg M (2017) UCP1 - A sophisticated energy valve. *Biochimie* 134:19-27.

- 1517 Koit A, Shevchuk I, Ounpuu L, Klepinin A, Chekulayev V, Timohhina N, Tepp K, Puurand M, Truu L, Heck K,
1518 Valvere V, Guzun R, Kaambre T (2017) Mitochondrial respiration in human colorectal and breast cancer
1519 clinical material is regulated differently. *Oxid Med Cell Longev* 1372640.
- 1520 Komlódi T, Tretter L (2017) Methylene blue stimulates substrate-level phosphorylation catalysed by succinyl-
1521 CoA ligase in the citric acid cycle. *Neuropharmacology* 123:287-98.
- 1522 Lane N (2005) *Power, sex, suicide: mitochondria and the meaning of life*. Oxford University Press:354 pp.
- 1523 Larsen S, Nielsen J, Neigaard Nielsen C, Nielsen LB, Wibrand F, Stride N, Schroder HD, Boushel RC, Helge
1524 JW, Dela F, Hey-Mogensen M (2012) Biomarkers of mitochondrial content in skeletal muscle of healthy
1525 young human subjects. *J Physiol* 590:3349-60.
- 1526 Lee C, Zeng J, Drew BG, Sallam T, Martin-Montalvo A, Wan J, Kim SJ, Mehta H, Hevener AL, de Cabo R,
1527 Cohen P (2015) The mitochondrial-derived peptide MOTS-c promotes metabolic homeostasis and reduces
1528 obesity and insulin resistance. *Cell Metab* 21:443-54.
- 1529 Lee SR, Kim HK, Song IS, Youm J, Dizon LA, Jeong SH, Ko TH, Heo HJ, Ko KS, Rhee BD, Kim N, Han J
1530 (2013) Glucocorticoids and their receptors: insights into specific roles in mitochondria. *Prog Biophys Mol*
1531 *Biol* 112:44-54.
- 1532 Leek BT, Mudaliar SR, Henry R, Mathieu-Costello O, Richardson RS (2001) Effect of acute exercise on citrate
1533 synthase activity in untrained and trained human skeletal muscle. *Am J Physiol Regul Integr Comp Physiol*
1534 280:R441-7.
- 1535 Lemieux H, Blier PU, Gnaiger E (2017) Remodeling pathway control of mitochondrial respiratory capacity by
1536 temperature in mouse heart: electron flow through the Q-junction in permeabilized fibers. *Sci Rep* 7:2840.
- 1537 Lenaz G, Tioli G, Falasca AI, Genova ML (2017) Respiratory supercomplexes in mitochondria. In: *Mechanisms*
1538 *of primary energy transduction in biology*. M Wikstrom (ed) Royal Society of Chemistry Publishing, London,
1539 UK:296-337.
- 1540 Margulis L (1970) *Origin of eukaryotic cells*. New Haven: Yale University Press.
- 1541 Meinild Lundby AK, Jacobs RA, Gehrig S, de Leur J, Hauser M, Bonne TC, Flück D, Dandanell S, Kirk N,
1542 Kaech A, Ziegler U, Larsen S, Lundby C (2017) Exercise training increases skeletal muscle mitochondrial
1543 volume density by enlargement of existing mitochondria and not de novo biogenesis. *Acta Physiol (Oxf)*
1544 [Epub ahead of print].
- 1545 Menshikova EV, Ritov VB, Fairfull L, Ferrell RE, Kelley DE, Goodpaster BH (2006) Effects of exercise on
1546 mitochondrial content and function in aging human skeletal muscle. *J Gerontol A Biol Sci Med Sci* 61:534-
1547 40.
- 1548 Menshikova EV, Ritov VB, Ferrell RE, Azuma K, Goodpaster BH, Kelley DE (2007) Characteristics of skeletal
1549 muscle mitochondrial biogenesis induced by moderate-intensity exercise and weight loss in obesity. *J Appl*
1550 *Physiol* (1985) 103:21-7.
- 1551 Menshikova EV, Ritov VB, Toledo FG, Ferrell RE, Goodpaster BH, Kelley DE (2005) Effects of weight loss
1552 and physical activity on skeletal muscle mitochondrial function in obesity. *Am J Physiol Endocrinol Metab*
1553 288:E818-25.
- 1554 Miller GA (1991) *The science of words*. Scientific American Library New York:276 pp. Mitchell P (1961)
1555 Coupling of phosphorylation to electron and hydrogen transfer by a chemi-osmotic type of mechanism.
1556 *Nature* 191:144-8.
- 1557 Mitchell P (2011) Chemiosmotic coupling in oxidative and photosynthetic phosphorylation. *Biochim Biophys*
1558 *Acta Bioenergetics* 1807:1507-38.
- 1559 Mitchell P, Moyle J (1967) Respiration-driven proton translocation in rat liver mitochondria. *Biochem J*
1560 105:1147-62.
- 1561 Mogensen M, Sahlin K, Fernström M, Glintborg D, Vind BF, Beck-Nielsen H, Højlund K (2007) Mitochondrial
1562 respiration is decreased in skeletal muscle of patients with type 2 diabetes. *Diabetes* 56:1592-9.
- 1563 Moreno M, Giacco A, Di Munno C, Goglia F (2017) Direct and rapid effects of 3,5-diiodo-L-thyronine (T2).
1564 *Mol Cell Endocrinol* 7207:30092-8.
- 1565 Morrow RM, Picard M, Derbeneva O, Leipzig J, McManus MJ, Gousspillou G, Barbat-Artigas S, Dos Santos C,
1566 Hepple RT, Murdock DG, Wallace DC (2017) Mitochondrial energy deficiency leads to hyperproliferation of
1567 skeletal muscle mitochondria and enhanced insulin sensitivity. *Proc Natl Acad Sci U S A* 114:2705-10.
- 1568 Paradies G, Paradies V, De Benedictis V, Ruggiero FM, Petrosillo G (2014) Functional role of cardiolipin in
1569 mitochondrial bioenergetics. *Biochim Biophys Acta* 1837:408-17.
- 1570 Pesta D, Hoppel F, Macek C, Messner H, Faulhaber M, Kobel C, Parson W, Burtcher M, Schocke M, Gnaiger
1571 E (2011) Similar qualitative and quantitative changes of mitochondrial respiration following strength and
1572 endurance training in normoxia and hypoxia in sedentary humans. *Am J Physiol Regul Integr Comp Physiol*
1573 301:R1078-87.
- 1574 Price TM, Dai Q (2015) The role of a mitochondrial progesterone receptor (PR-M) in progesterone action.
1575 *Semin Reprod Med* 33:185-94.
- 1576 Prigogine I (1967) *Introduction to thermodynamics of irreversible processes*. Interscience, New York, 3rd
1577 ed:147pp.

- 1578 Puchowicz MA, Varnes ME, Cohen BH, Friedman NR, Kerr DS, Hoppel CL (2004) Oxidative phosphorylation
 1579 analysis: assessing the integrated functional activity of human skeletal muscle mitochondria – case studies.
 1580 Mitochondrion 4:377-85. Puntschart A, Claassen H, Jostarndt K, Hoppeler H, Billeter R (1995) mRNAs of
 1581 enzymes involved in energy metabolism and mtDNA are increased in endurance-trained athletes. Am J
 1582 Physiol 269:C619-25.
- 1583 Quiros PM, Mottis A, Auwerx J (2016) Mitonuclear communication in homeostasis and stress. Nat Rev Mol
 1584 Cell Biol 17:213-26.
- 1585 Reichmann H, Hoppeler H, Mathieu-Costello O, von Bergen F, Pette D (1985) Biochemical and ultrastructural
 1586 changes of skeletal muscle mitochondria after chronic electrical stimulation in rabbits. Pflugers Arch 404:1-
 1587 9.
- 1588 Renner K, Amberger A, Konwalinka G, Gnaiger E (2003) Changes of mitochondrial respiration, mitochondrial
 1589 content and cell size after induction of apoptosis in leukemia cells. Biochim Biophys Acta 1642:115-23.
- 1590 Rich P (2003) Chemiosmotic coupling: The cost of living. Nature 421:583.
- 1591 Rostovtseva TK, Sheldon KL, Hassanzadeh E, Monge C, Saks V, Bezrukov SM, Sackett DL (2008) Tubulin
 1592 binding blocks mitochondrial voltage-dependent anion channel and regulates respiration. Proc Natl Acad Sci
 1593 USA 105:18746-51.
- 1594 Rustin P, Parfait B, Chretien D, Bourgeron T, Djouadi F, Bastin J, Rötig A, Munnich A (1996) Fluxes of
 1595 nicotinamide adenine dinucleotides through mitochondrial membranes in human cultured cells. J Biol Chem
 1596 271:14785-90.
- 1597 Saks VA, Veksler VI, Kuznetsov AV, Kay L, Sikk P, Tiivel T, Tranqui L, Olivares J, Winkler K, Wiedemann F,
 1598 Kunz WS (1998) Permeabilised cell and skinned fiber techniques in studies of mitochondrial function in
 1599 vivo. Mol Cell Biochem 184:81-100.
- 1600 Salabei JK, Gibb AA, Hill BG (2014) Comprehensive measurement of respiratory activity in permeabilized cells
 1601 using extracellular flux analysis. Nat Protoc 9:421-38.
- 1602 Sazanov LA (2015) A giant molecular proton pump: structure and mechanism of respiratory complex I. Nat Rev
 1603 Mol Cell Biol 16:375-88.
- 1604 Schneider TD (2006) Claude Shannon: biologist. The founder of information theory used biology to formulate
 1605 the channel capacity. IEEE Eng Med Biol Mag 25:30-3.
- 1606 Schönfeld P, Dymkowska D, Wojtczak L (2009) Acyl-CoA-induced generation of reactive oxygen species in
 1607 mitochondrial preparations is due to the presence of peroxisomes. Free Radic Biol Med 47:503-9.
- 1608 Schrödinger E (1944) What is life? The physical aspect of the living cell. Cambridge Univ Press.
- 1609 Schultz J, Wiesner RJ (2000) Proliferation of mitochondria in chronically stimulated rabbit skeletal muscle--
 1610 transcription of mitochondrial genes and copy number of mitochondrial DNA. J Bioenerg Biomembr 32:627-
 1611 34.
- 1612 Simson P, Jepihhina N, Laasmaa M, Peterson P, Birkedal R, Vendelin M (2016) Restricted ADP movement in
 1613 cardiomyocytes: Cytosolic diffusion obstacles are complemented with a small number of open mitochondrial
 1614 voltage-dependent anion channels. J Mol Cell Cardiol 97:197-203.
- 1615 Stucki JW, Ineichen EA (1974) Energy dissipation by calcium recycling and the efficiency of calcium transport
 1616 in rat-liver mitochondria. Eur J Biochem 48:365-75.
- 1617 Tonkonogi M, Harris B, Sahlin K (1997) Increased activity of citrate synthase in human skeletal muscle after a
 1618 single bout of prolonged exercise. Acta Physiol Scand 161:435-6.
- 1619 Waczulikova I, Habodaszova D, Cagalinec M, Ferko M, Ulicna O, Mateasik A, Sikurova L, Ziegelhöffer A
 1620 (2007) Mitochondrial membrane fluidity, potential, and calcium transients in the myocardium from acute
 1621 diabetic rats. Can J Physiol Pharmacol 85:372-81.
- 1622 Wagner BA, Venkataraman S, Buettner GR (2011) The rate of oxygen utilization by cells. Free Radic Biol Med
 1623 51:700-712.
- 1624 Wang H, Hiatt WR, Barstow TJ, Brass EP (1999) Relationships between muscle mitochondrial DNA content,
 1625 mitochondrial enzyme activity and oxidative capacity in man: alterations with disease. Eur J Appl Physiol
 1626 Occup Physiol 80:22-7.
- 1627 Wang T (2010) Coulomb force as an entropic force. Phys Rev D 81:104045.
- 1628 Watt IN, Montgomery MG, Runswick MJ, Leslie AG, Walker JE (2010) Bioenergetic cost of making an
 1629 adenosine triphosphate molecule in animal mitochondria. Proc Natl Acad Sci U S A 107:16823-7.
- 1630 Weibel ER, Hoppeler H (2005) Exercise-induced maximal metabolic rate scales with muscle aerobic capacity. J
 1631 Exp Biol 208:1635-44.
- 1632 White DJ, Wolff JN, Pierson M, Gemmell NJ (2008) Revealing the hidden complexities of mtDNA inheritance.
 1633 Mol Ecol 17:4925-42.
- 1634 Wikström M, Hummer G (2012) Stoichiometry of proton translocation by respiratory complex I and its
 1635 mechanistic implications. Proc Natl Acad Sci U S A 109:4431-6.
- 1636 Willis WT, Jackman MR, Messer JI, Kuzmiak-Glancy S, Glancy B (2016) A simple hydraulic analog model of
 1637 oxidative phosphorylation. Med Sci Sports Exerc 48:990-1000.